Mathematics MSc Dissertation MTHM038, 2019/20

Synchronisation of Coupled Nonlinear Oscillators in the Kuramoto Model

A numerical and analytical exploration

Mark Baldwin, ID 180989331

Supervisor: Dr. Wolfram Just

A thesis presented for the degree of
Master of Science in *Mathematics*

School of Mathematical Sciences
Queen Mary University of London

Declaration of original work

This declaration is made on September 8, 2020.

Student's Declaration:

I, Mark Baldwin, hereby declare that the work in this thesis is my original work. I have not copied from any other students' work, work of mine submitted elsewhere, or from any other sources except where due reference or acknowledgement is made explicitly in the text, nor has any part been written for me by another person.

Referenced text has been flagged by:

1. Using italic fonts, **and**
2. using quotation marks "...", **and**
3. explicitly mentioning the source in the text.

Acknowledgements

I would like to thank Dr Wolfram Just for some very useful guidance pointing me in the right direction at various stages of the project, as well as providing positive and critical feedback when it was needed.

Abstract

The spontaneous synchronisation of large populations of coupled, nonlinear, limit-cycle oscillators has attracted a great deal of attention in the last few decades. This phenomenon is observed in a large variety of biological, chemical, physical and social systems. One successful attempt to attack this problem is the Kuraomoto model, where each of the oscillators is modelled as a phase oscillator interacting in a variety of ways with some or all of the oscillators in the population. This work explores some of the fundamental properties of the Kuramoto model through both theoretical analysis as well as numerical simulation. We begin by reworking Kuramoto's original analysis for a population of globally coupled oscillators, and find that in the infinite population continuum limit, a phase transition occurs whereby some or all of the oscillators spontaneously synchronise if the coupling is sufficiently strong. We use numerical integration to explore the dynamics of a finite population of oscillators and find good comparison with theoretical predictions. We explore all regions of the stability diagram to establish the stability or instability of the various branches of the bifurcation curve and provide numerical evidence of a second-order phase transition to synchronisation in the system. The model is adapted by introducing a frustration parameter into the coupling through a constant phase-shift. The so called Kuramoto-Sakaguchi model is examined on a one-dimension ring network where the coupling is non-local. For a finite population of identical oscillators surprising dynamics are observed. For certain parameter values the formation of both synchronised and incoherent states coexisting on the network is observed. These so called "Chimera" states are shown to be sensitive to initial conditions and we briefly explore their stability over long time scales numerically. Although inconclusive, they do not appear to be stable entities over long time scales, at least for the finite population size simulations performed here.

Contents

Chapter 1

Introduction and motivation

1.1 Historical overview

Collective synchronisation whereby a large system of interacting elements adjust their rhythm to oscillate at the same frequency, although each oscillator has its own preferred natural frequency, is ubiquitous in nature (Strogatz and Stewart, 1993; Strogatz, 2000; Pikovsky et al., 2001; Acebrón et al., 2005).

The first recorded observation of synchronous behaviour was made by Christiaan Huygens while observation the motion of two pendulum clocks and is recorded in a letter to his father on 26 February 1665 while sick in bed (Pikovsky et al., 2001; Huygens, 1967):

> "*While I was forced to stay in bed for a few days and made observations on my two clocks of the new workshop, I noticed a wonderful effect that nobody could have thought of before. The two clocks, while hanging [on the wall] side by side with a distance of one or two feet between, kept in pace relative to each other with a precision so high that the two pendulums always swung together, and never varied. While I admired this for some time, I finally found that this happened due to a sort of* sympathy*: when I made the pendulums swing at differing paces, I found that half an hour later, they always returned to synchronism and kept it constantly afterwards, as long as I let them go. Then, I put them further away from one another, hanging one on one side of the room and the other one fifteen feet away. I saw that after one day, there was a*

> *difference of five seconds between them and, consequently, their earlier agreement was only due to some sympathy that, in my opinion, cannot be caused by anything other than the imperceptible stirring of the air due to the motion of the pendulums.*"

Furthermore, Huygens discovered that this state was stable:

> *"...further, if this agreement was disturbed by some interference, it established itself in a short time.*".

He sought to explain the *"sympathy of the two clocks"* and realised that the clocks were synchronised due to the coupling provided by the movement of the supporting beam although it was hardly perceptible.

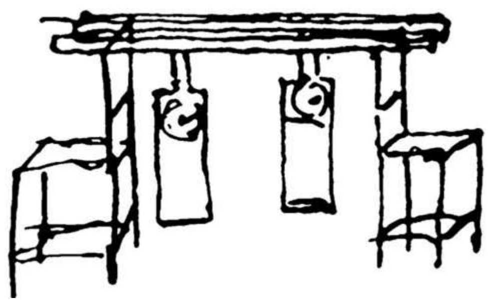

Figure 1.1: Illustration of Huygens experiments with two pendulum clocks with common support. (Pikovsky et al., 2001)

Synchronisation is observed in a huge variety of natural situations and over a wide range of time scales. In biological systems the synchronous flashing of fireflies (Buck, 1988) can be observed as well as the synchronised firing of pacemaker cells in the heart (Winfree, 2001). In social systems we can observe synchronised applause (Néda et al., 2000) and there is a huge volume of research now on neural synchronisation in the brain (Gray, 1994; Izhikevich, 2007; MacKay, 1997). There are many engineering examples, for example synchronisation in power grids (Filatrella et al., 2008; Rohden et al., 2012), in laser arrays (Blackbeard et al., 2014) and numersous examples in other fields such as electronics, meteorology, economics and chemistry (Strogatz, 2004).

All of these examples have one thing in common. Each of the individual oscillating units has its own preferred frequency with which to oscillate. No single oscillator is 'in charge' directing the rest of the population. It is the collective behaviour and interaction among the population that leads to the emergence of collective oscillations that synchronise.

The first mathematical study of this phenomenon was carried out by Wiener (1958, 1961) investigating alpha brain wave oscillations. However the model proved to be intractable mathematically and was not developed further. Winfree (1967) was the first to put the problem on a firm mathematical footing by treating the population as a large system of weakly interacting phase oscillators. He observed, through simulation, that the oscillations would synchronise spontaneously with sufficiently strong coupling. However the model still proved to be intractable to all but this simplest of situations. Inspired by Winfree's work, Kuramoto (1975) made simplifications and produced a more tractable model that we investigate here.

1.2 Thesis overview

In this work we explore the model suggested by Kuramoto, and modifications to it. We begin with a mathematical introduction and show that a system of Stuart-Landau oscillators, under certain assumptions, can be modelled as a population of phase oscillators. In fact, (Kuramoto, 1975) showed that any system of weakly coupled, identical self sustained oscillators the dynamics can be reduced to interacting phase equations.

We derive the key properties of a globally coupled infinite population in a continuum formulation and then explore a finite population through numerical simulation. The effect of the distribution of natural frequencies as well as coupling strength is explored numerically.

We then consider an interesting modification to the original model and explore the dynamics on a finite one-dimensional ring network and also introduce non-local couple between the oscillators.

All numerical integrations are coded in Matlab using the inbuilt `ode45` routine. This is an embedded Runge-Kutta (4,5) routine which has adaptive step size control and was found to be suitable for all integrations in this work.

Chapter 2

Synchronisation of coupled oscillators

2.1 Populations of limit cycle oscillators

One of the earliest successful attempts to describe synchronous behaviour in a mathematical way was made by Winfree (1967). Winfree considered a large population of identical weakly interacting limit-cycle oscillators. The dynamics of each oscillator is described only by its phase on a short timescale. On longer timescales, the key is to consider each oscillator coupled to an overall *mean-field* generated by all the oscillators (Strogatz, 2004, 2000). In Winfree's model, the evolution of the phase of each oscillator is governed by

$$\dot{\theta}_i = \omega_i + \left(\sum_{j=1}^{N} X(\theta_j) \right) Z(\theta_i), \quad i = 1, \dots N, \tag{2.1}$$

where θ_i is the phase of each oscillator, ω_i its natural frequency. Each oscillator influences the collective mean-field through X and responds to it through Z. Winfree had some success with numerical simulation of (2.1) and discovered synchronisation could occur with sufficiently large coupling.

Motivated by Winfree's work, Kuramoto (1975) considered a simpler model for the dynamics of a single self-sustained oscillator that is governed by the Stuart-Landau equation

$$\frac{\mathrm{d}Q}{\mathrm{d}t} = i\omega Q + (\alpha - \beta|Q|^2)Q \tag{2.2}$$

with $\alpha, \beta > 0$, which describes the dynamics near to a Hopf bifurcation. Writing the complex variable Q as, $Q = \rho e^{i\theta}$ and substituting into (2.2) we get

$$i\rho e^{i\theta}\frac{\mathrm{d}\theta}{\mathrm{d}t} + \frac{\mathrm{d}\rho}{\mathrm{d}t}e^{i\theta} = i\omega\rho e^{i\theta} + (\alpha - \beta\rho^2)\rho e^{i\theta} \tag{2.3}$$

Equating real parts we get

$$\frac{\mathrm{d}\rho}{\mathrm{d}t} = (\alpha - \beta\rho^2) \tag{2.4}$$

and so ρ has a stable fixed point $\rho_s = \sqrt{\alpha/\beta}$. Equating imaginary parts gives

$$\frac{\mathrm{d}\theta}{\mathrm{d}t} = \omega \tag{2.5}$$

Assigning ρ to this fixed value ρ_s we see that we get a self-sustained limit cycle with amplitude ρ_s and phase θ varying with time given by (2.5). This is shown in Fig. 2.1. Kuramoto then considered a population of N interacting Stuart-Landau

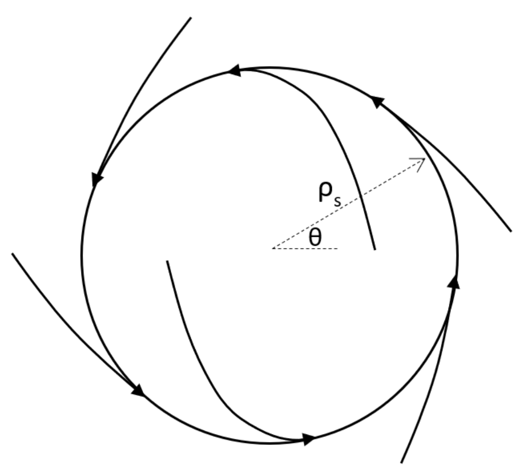

Figure 2.1: Limit cycle of the Stuart-Landau oscillator. This represents the motion of a single self-sustained oscillator in (ρ, θ) space. ρ remains constant and so the limit cycle is a circle. The limit cycle is stable, so any trajectory that starts away from the limit cycle approaches it asymptotically.

oscillators where each oscillator has its own frequency and interacts with every other oscillator. This can be modelled as

$$\frac{\mathrm{d}Q_i}{\mathrm{d}t} = i\omega_i Q_i + (\alpha - \beta|Q|^2)Q_i + \sum_{j=1,j\neq i}^{N} K_{ij}Q_{ij} \tag{2.6}$$

In considering the system defined in (2.6) in a similar way to the single oscillator situation, Kuramoto made some simplifying assumptions:

1. $K_{ij} = K/N$
2. $N \to \infty$
3. $\alpha, \beta \to \infty$, while $\alpha/\beta, \omega_i, K$ remain finite

The implication for the scaling of the coupling K_{ij} is that there is constant *all-to-all* coupling between each oscillator that is *weak*. In a similar fashion to the single oscillator case, we write $Q_i = \rho_i e^{i\theta_i}$ and substitute into (2.6). Owing to assumption (3) it is easy to see that ρ_i will reach a constant value $\rho_{si} = \sqrt{\alpha/\beta}$, $\forall i$ over time as with the single oscillator case. Consequently equating imaginary parts of (2.6) on the limit cycles $\rho_i = \rho_{si}$ leads to

$$\frac{\mathrm{d}\theta_i}{\mathrm{d}t} = \omega_i + \frac{K}{N}\sum_{j=1}^{N} \sin(\theta_j - \theta_i) \tag{2.7}$$

which is the Kuramoto model for a population of N oscillators with global all-to-all coupling. It is this model that we will begin to explore analytically in the next chapter as a basic model for synchronisation in a population of coupled limit cycle oscillators..

2.2 Definition of synchronisation

As outlined in section 1.1, oscillators in the real world can often interact and synchronise with each other. Before we proceed with a in-depth exploration of the dynamics exhibited by (2.7) it is worthwhile to briefly outline the meaning of synchronisation in a more rigorous way.

Here we focus on the dynamics of a population of N oscillators as defined by (2.7). However the same arguments would apply to different models of synchronisation.

Each phase variable, $\theta_i(t)$, is 2π-periodic and is defined on the unit circle $\mathbb{S}^1$. Since there are N oscillators, the state space of this systems is the N-torus, $\mathbb{T}^N = \mathbb{S}^1 \times \ldots \times \mathbb{S}^1$. *Frequency locking* is said to occur when there is a periodic trajectory on this N-torus.

For example, in the case of two oscillators if θ_1 rotates p times around the torus and θ_2 rotates q times, then we have $p : q$ frequency locking if p/q is rational. If p/q is irrational then*quasi-periodic* motion will occur.

If the two oscillators are frequency-locked then they can be said to be *phased-locked* if $q\dot{\theta}_1(t) = p\dot{\theta}_2(t)$. The oscillators are said to be *synchronised* if they are 1:1 phased-locked, $\dot{\theta}_1(t) = \dot{\theta}_2(t)$.

So for our original population of N oscillators, they are fully synchronised when all oscillators are 1:1 phase-locked. There may be *partial synchronisation* where only a subset of the N oscillators are synchronised. Figure 2.2 shows pictorially the relationship between these definitions.

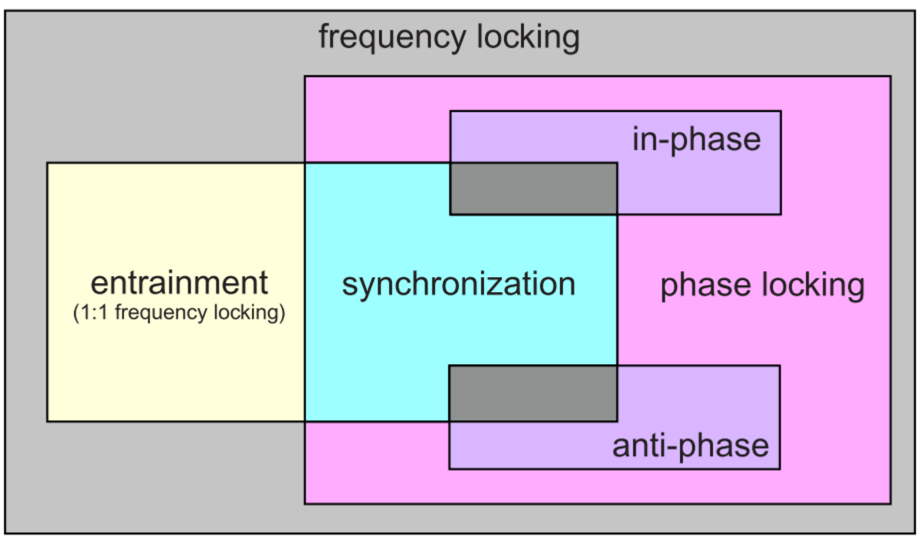

Figure 2.2: Various degrees of locking of oscillators. Taken from (Izhikevich, 2007).

Chapter 3

The Kuramoto model with global coupling

3.1 The mean-field and the order parameter

As outlined in section 2.1 the dynamics of a large number, N, of self sustained limit cycle oscillators can be described by the Kuramoto model through a system of first order differential equations (3.1) in $\mathbb{R}^N$, governing the evolution of the phase $\theta_i(t)$, of each oscillator, which resides on a unit circle.

$$\begin{aligned} \dot{\theta}_i(t) &= \omega_i + \frac{K}{N}\sum_{j=1}^{N}\sin(\theta_j(t)-\theta_i(t)) \quad i=1,\ldots N, \\ \theta_i(0) &= \theta_{0i} \end{aligned} \tag{3.1}$$

Each oscillator has its own natural oscillating frequency ω_i, which is drawn randomly from some specified distribution $g(\omega)$ (specifically a probability density) with normalisation $\int_{-\infty}^{\infty} g(\omega)\mathrm{d}\omega = 1$. In the case considered here, $K \geq 0$ represents a constant coupling parameter and the appearance of the factor $1/N$ is to ensure the model remains well behaved in the limit $N \to \infty$. Equation 3.1 describes the *globally coupled* or *all-to-all coupled* Kuramoto model where each oscillator is coupled to every other oscillator through a constant coupling parameter. Figure 3.1 visualises the situation for $N = 4$ oscillators with *all-to-all* coupling. Each oscillator resides at the node of a *complete network* and consequently is connected to every other oscillator. The distribution of ω_i introduces randomness into the model, whereas the summation term on the r.h.s of (3.1) attempts the bring each oscillator in phase through attractive coupling.

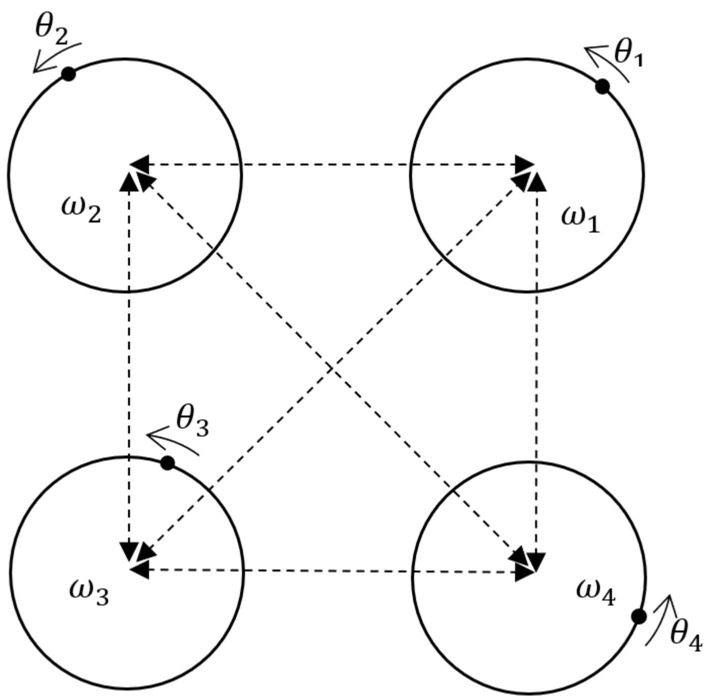

Figure 3.1: Visualisation of the globally coupled Kuramoto model for a network of $N = 4$ oscillators. Each oscillator is coupled to every other oscillator through an *all-to-all* coupling.

With all coupling removed $K = 0$ it is easy to see that each oscillator's phase evolves independently of all the others, at its intrinsic frequency ω_i as in (3.2).

$$\dot{\theta}_i(t) = \omega_i, \quad i = 1, \dots N. \tag{3.2}$$

In effect then, each oscillator tries to run independently of all the others but is drawn through the sinusoidal couple term to synchronise to all others.

Kuramoto's original analysis (Kuramoto, 1983; Acebrón et al., 2005; Strogatz, 2000), assumed that the distribution of intrinsic frequencies $g(\omega)$ is unimodal and is also symmetric about the mean frequency $\langle\omega\rangle = \Omega$. That is,

$$g(\Omega + \omega) = g(\Omega - \omega), \tag{3.3}$$

where Ω is given by

$$\Omega = \int_{-\infty}^{\infty} \omega g(\omega) d\omega \tag{3.4}$$

By making the transformation $\theta_i(t) \to \theta_i(t) + \Omega t$, (3.1) remains invariant but with intrinsic frequencies $\omega_i - \Omega$. So without loss of generality we can set $\Omega = 0$ which physically means moving into a frame rotating with the mean frequency Ω. This shifts the mean of $g(\omega)$ to zero and consequently the symmetry,

$$g(\omega) = g(-\omega) \tag{3.5}$$

Next we follow Kuramoto's original self-consistent analysis (Kuramoto, 1983; Acebrón et al., 2005; Gupta et al., 2014) to attempt to establish some analytical results concerning the emergence of synchronous behaviour in the system (3.1).

To start with, a complex *order parameter*

$$r(t)\mathrm{e}^{i\psi(t)} = \frac{1}{N}\sum_{j=1}^{N} \mathrm{e}^{i\theta_j(t)}, \tag{3.6}$$

is defined. This can be thought of as macroscopic average that describes the overall dynamics of the entire population of oscillators. If the phase of each oscillator is visualised as a collection of points moving around a unit circle each with a corresponding unit vector pointing to each, then $\psi(t)$ describes the average phase and $r(t)$ describes the coherence of the phases. The complex order parameter, (3.6) can be thought of as describing the 'centre of mass' of the phases as they move around the circle.

Kuramoto uses $r(t)$ as a measure of the degree of synchrony of the systems of oscillators. If $r(t) = 0$ then the phases are scattered uniformly around the circle and there is no coherence or *complete incoherence*. In the extreme case where all phases have the same value, $r(t) = 1$ and their is *complete synchronisation*. If $r(t) > 0$ there is clustering of the phases. Some oscillators whose natural frequencies are close to the average frequency become *phase locked* at the average phase $\psi(t)$ and will rotate around the circle with frequency Ω, the remaining oscillators form a set of *drifting* oscillators moving of their own accord around the circle. This is a state of *partial synchronisation*.

Figure (3.2) provides a visualisation of the order parameter for a network of

$N = 8$ oscillators. In introducing the order parameter (3.6), we can think of it as

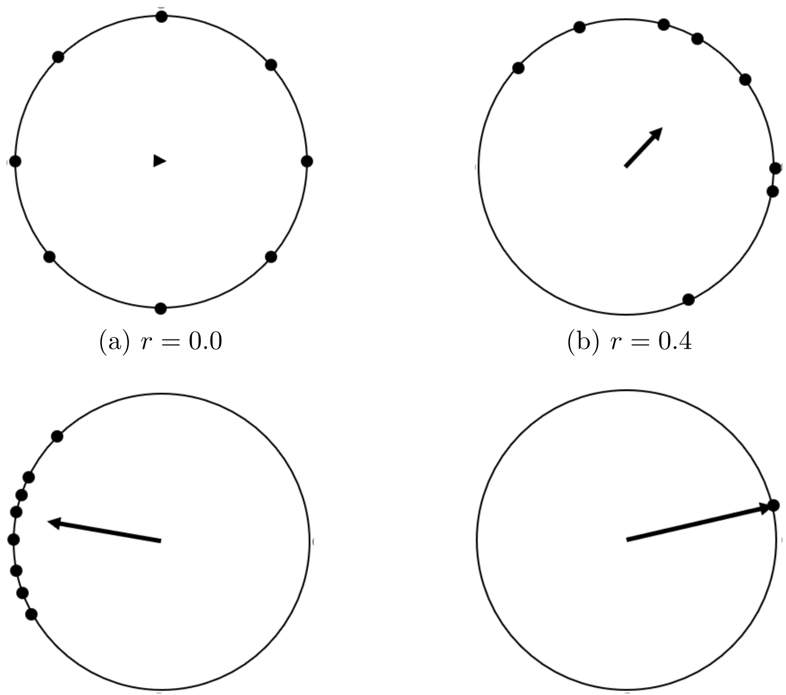

(a) $r = 0.0$ (b) $r = 0.4$ (c) $r = 0.8$ (d) $r = 1.0$

Figure 3.2: Visualising the order parameter for $N = 8$ oscillators. Points on the unit circle represent the phase, θ_j, of each oscillator. The 'center of mass' of the phases is represented by the complex number $re^{i\psi}$ and is visualised by the vector of length r and angular displacement ψ. For $r = 0$ the points are distributed uniformly around the unit circle. As r increases they cluster more, until when $r = 1$ all oscillators have identical phases.

describing the *mean field* of the system (3.1).

It will be useful to now redefine the original system (3.1) in terms of the mean field parameters r and ψ. To this end we first multiply (3.6) through by $e^{-i\theta}$

$$re^{i(\psi-\theta_i)} = \frac{1}{N}\sum_{j=1}^{N} e^{i(\theta_j-\theta_i)}, \quad i = 1, \dots N, \tag{3.7}$$

Equating the imaginary parts of (3.7) we get

$$\mathrm{Im}\left(re^{i(\psi-\theta_i)}\right) = \mathrm{Im}\left(\frac{1}{N}\sum_{j=1}^{N} e^{i(\theta_j-\theta_i)}\right), \quad i = 1, \dots N, \tag{3.8}$$

and so

$$r\sin(\psi - \theta_i) = \frac{1}{N}\sum_{j=1}^{N}\sin(\theta_j - \theta_i), \quad i = 1, \dots N, \tag{3.9}$$

Noticing the form of the r.h.s. of (3.9) we can substitute directly into the original equations of motion (3.1) to obtain

$$\dot{\theta} = \omega_i + Kr\sin(\psi - \theta_i), \quad i = 1, \dots N, \tag{3.10}$$

Equation 3.10 describes the system as a mean field model. The oscillators appear uncoupled, however each oscillator is coupled to every other oscillator through the mean field quantities r and ψ. Each oscillator is attracted to the average phase of the combined population through ψ. The strength of this attraction is proportional to Kr.

This mean field description of the coupling can explain the basic mechanism behind synchronisation. As the phases become more clustered r increases, leading to increased coherence and clustering, subsequently increasing r further, and so on.

If K is too small however it is possible that that oscillators will not synchronise their phases as the second term on the r.h.s of (3.10) could become negligible and the evolution of θ_i would be dominated by the ω_i term. Alternatively for strong coupling $K \gg 0$, it is possible that all phases have a dominant attraction to the collective mean phase and synchronise to it. As we will show, there a critical value of the coupling constant K_c that depends on the initial distribution of frequencies $g(\omega)$ below which this synchronisation will not occur.

We will investigate the form his critical coupling takes analytically in the following sections and explore this further numerically in Chapter 4.

In order to obtain more concrete mathematical description of the behaviour of $r(t)$ and to obtain a measure for the critical coupling parameter, we follow Kuramomto's original development and introduce a continuum description of the problem in the limit $N \to \infty$.

3.2 The continuum limit

To explore the dynamics of (3.1) or (3.10), for example to establish the behaviour of $r(t)$ as $t \to \infty$ or to analyse the stability of the stationary solutions in the finite

N formulation, is difficult, if not impossible. In order to gain any traction on the analysis of (3.1) it is useful to use a statistical physics approach and to re-cast the entire problem in the continuum limit as $N \to \infty$, as would be done in the kinetic theory of gases for example. The system is then cast into a continuous form in terms of *densities* (Strogatz, 2000; Gupta et al., 2018).

In this case we assume an infinite continuum of oscillators spread over the unit circle. We introduce the density function $\rho(\theta, \omega, t)$, where $\rho(\theta, \omega, t)\mathrm{d}\theta$ gives the fraction of oscillators with natural frequency ω whose phase lies between θ and $\theta + \mathrm{d}\theta$ at time t. We note that ρ is non-negative and periodic such that

$$\rho(\theta + 2\pi, \omega, t) = \rho(\theta, \omega, t) \tag{3.11}$$

as is normalised such that

$$\int_0^{2\pi} \rho(\theta, \omega, t)\mathrm{d}\theta = 1 \tag{3.12}$$

Oscillators are neither created nor destroyed and so the number of oscillators with the same natural frequency has to be conserved in time. The *conservation of oscillators* is then expressed as

$$\frac{\partial \rho}{\partial t} = -\frac{\partial}{\partial t}\left(\rho v\right) \tag{3.13}$$

which describes the evolution of ρ over time. Equation (3.13) expresses the fact that if ρ, the density of oscillators of frequency ω, changes at a particular location (a certain phase) on the unit circle, then this is compensated for by a flux of oscillators from elsewhere on the circle. Here v is the *velocity* of an oscillator at *position* θ and natural frequency ω. From (3.10) we see that

$$v(\theta, \omega, t) = \dot{\theta} = \omega + Kr(t)\sin(\psi - \theta), \tag{3.14}$$

Where the order parameter, given by (3.6), is now expressed as

$$r(t)e^{i\psi(t)} = \int_0^{2\pi}\int_{-\infty}^{\infty} e^{i\theta}\rho(\theta, \omega, t)g(\omega)\mathrm{d}\omega\mathrm{d}\theta, \tag{3.15}$$

in the continuum limit. Substituting (3.14) into (3.13) leads to

$$\frac{\partial \rho}{\partial t} = -\frac{\partial}{\partial \theta}\left[\rho\left(\omega + Kr(t)\sin(\psi - \theta)\right)\right] \tag{3.16}$$

Further substituting (3.15) into (3.16) leads, after some simple algebra (Strogatz, 2000; Gupta et al., 2018), to

$$\frac{\partial \rho}{\partial t} = -\frac{\partial}{\partial \theta}\left[\rho\left(\omega + K\int_0^{2\pi}\int_{-\infty}^{\infty}\sin(\theta' - \theta)\rho(\theta', \omega', t)g(\omega')\mathrm{d}\omega'\mathrm{d}\theta'\right)\right] \tag{3.17}$$

Equation (3.17) represents the Kuramoto model (3.1) in the continuum limit $N \to \infty$.

3.3 Fixed points and Kuramoto's solution

Note that (3.11)-(3.17) has a trivial stationary ($\partial_t = 0$) solution

$$\rho(\theta, \omega) = \frac{1}{2\pi}, \quad r = 0 \tag{3.18}$$

which corresponds to the completely incoherent state. In this state, for each ω, all oscillator phases are even distributed around the unit circle. Strogatz and Mirollo (1991) performed a linear stability analysis of this state. They found that it is unstable when K is above some critical value K_c and neutrally stable when $K < K_c$. This confirmed an original hypothesis of Kuramoto (1983), that the incoherent state becomes unstable when $K > K_c$.

In his original analysis, Kuramoto (1983) argued that over long time periods, after the decay of transients, both r and ψ would remain constant. In fact, ψ would rotate at the constant frequency Ω. Returning to (3.10) and making $\dot{r} = 0$ and moving to a frame rotating with frequency Ω, we can make $\psi = 0$ without loss of generality to get,

$$\dot{\theta} = \omega_i - Kr\sin(\theta_i), \quad i = 1, \ldots N, \tag{3.19}$$

We need to look at solutions to this, which will be dependent on r. The resulting solutions will in turn modify r and ψ which then need to be consistent with the original definition of the order parameter (3.6). This is the self-consistent analysis

Kuramoto undertook. Note that a stable fixed point exists if $|\omega_i| \leq Kr$ and is given by solutions to

$$\omega_i = Kr \sin\theta_i \tag{3.20}$$

These represent oscillators that are *phased locked* in this rotating frame. If $|\omega_i| > Kr$ then (3.19) does not posses a fixed point. Kuramoto demanded that these *drifting oscillators* formed a stationary state on the circle in order for both r and ψ to remain constant. The effect of this is that the 'center of mass' of the phases of the drifting oscillators, given by the order parameter, remains fixed. Under this assumption we have $\partial\rho/\partial t = 0$ and (3.13) becomes

$$\rho(\theta,\omega)v(\theta,\omega) = C(\omega) \tag{3.21}$$

where $C(\omega)$ is an ω-dependent constant. This leads to an expression for ρ

$$\rho(\theta,\omega) = \frac{C(\omega)}{|\dot{\theta}|} = \frac{C(\omega)}{|\omega - Kr\sin\theta|} \tag{3.22}$$

Normalisation requires that:

$$\int_{-\pi}^{\pi} \rho(\theta,\omega)d\theta = C(\omega)\int_{-\pi}^{\pi} \frac{d\theta}{|\omega - Kr\sin\theta|} = 1 \tag{3.23}$$

leading to (Acebrón et al., 2005; Strogatz, 2000)

$$C(\omega) = \frac{1}{2\pi}\sqrt{\omega^2 - (Kr)^2} \tag{3.24}$$

Hence we obtain the full solution describing partial synchronisation:

$$\rho(\theta,\omega) = \begin{cases} \delta(\theta - \arcsin(\frac{\omega}{Kr})), & |\omega| \leq Kr, \quad \textit{locked} \\ \frac{\sqrt{\omega^2 - (Kr)^2}}{2\pi|\omega - Kr\sin\theta|}, & |\omega| > Kr, \quad \textit{drifting} \end{cases} \tag{3.25}$$

We would now like to evaluate the order parameter for this state of partial synchronisation. Returning to the order parameter defined in the limit $N \to \infty$ in (3.15)

$$r(t)e^{i\psi(t)} = \int_0^{2\pi}\int_{-\infty}^{\infty} e^{i\theta}\rho(\theta,\omega,t)g(\omega)\mathrm{d}\omega\mathrm{d}\theta,$$

We note that this is just an average of $e^{i\theta}$ over both phase and frequency. Hence

$$r(t)e^{i\psi(t)} = \langle e^{i\theta}\rangle = \langle e^{i\theta}\rangle_{\text{locked}} + \langle e^{i\theta}\rangle_{\text{drifting}} \tag{3.26}$$

However

$$\langle e^{i\theta}\rangle = re^{\psi} = r \tag{3.27}$$

as $\psi = 0$, and so

$$r = \langle \mathrm{e}^{i\theta}\rangle_{\text{locked}} + \langle \mathrm{e}^{i\theta}\rangle_{\text{drifting}} \tag{3.28}$$

We now follow and expand on the development given by Strogatz (2000); Acebrón et al. (2005); Gupta et al. (2014), to establish contributions to r from both the drifting and the locked oscillators.

Contribution of the *drifting* oscillators to the order parameter

In the drifting state $|w| > Kr$, so we integrate over the unit circle for these frequencies:

$$\langle \mathrm{e}^{i\theta}\rangle_{\text{drifting}} = \int_0^{2\pi}\int_{|\omega|>Kr} \rho(\theta,\omega)g(\omega)\mathrm{e}^{i\theta}d\omega d\theta \tag{3.29}$$

$$\langle \mathrm{e}^{i\theta}\rangle_{\text{drifting}} = \int_0^{2\pi}\int_{-\infty}^{-Kr} \rho(\theta,\omega)g(\omega)\mathrm{e}^{i\theta}d\omega d\theta + \int_0^{2\pi}\int_{Kr}^{\infty} \rho(\theta,\omega)g(\omega)\mathrm{e}^{i\theta}d\omega d\theta \tag{3.30}$$

Making a change of variable ($\omega \to -\omega$) to the first term of of (3.30) gives

$$\langle e^{i\theta}\rangle_{\text{drifting}} = -\int_0^{2\pi}\int_{\infty}^{Kr} \rho(\theta,-\omega)g(-\omega)\mathrm{e}^{i\theta}d\omega d\theta + \int_0^{2\pi}\int_{Kr}^{\infty} \rho(\theta,\omega)g(\omega)\mathrm{e}^{i\theta}d\omega d\theta \tag{3.31}$$

Making a further change of variable $\theta = \theta' + \pi$ to the first integral gives

$$\langle e^{i\theta}\rangle_{\text{drifting}} = -\int_{-\pi}^{\pi}\int_{\infty}^{Kr} \rho(\theta'+\pi,-\omega)g(-\omega)\mathrm{e}^{i(\theta'+\pi)}d\omega d\theta' + \int_0^{2\pi}\int_{Kr}^{\infty} \rho(\theta,\omega)g(\omega)\mathrm{e}^{i\theta}d\omega d\theta \tag{3.32}$$

Changing the order of the ω integration and noting that $e^{i\pi} = -1$ we get

$$\langle e^{i\theta}\rangle_{\text{drifting}} = -\int_{-\pi}^{\pi}\int_{Kr}^{\infty}\rho(\theta'+\pi,-\omega)g(-\omega)e^{i\theta'}d\omega d\theta' + \int_{0}^{2\pi}\int_{Kr}^{\infty}\rho(\theta,\omega)g(\omega)e^{i\theta}d\omega d\theta \tag{3.33}$$

Noting the symmetry, $g(\omega) = g(-\omega)$ from our initial assumption on the distribution, and als, $\rho(\theta+\pi,-\omega) = \rho(\theta,\omega)$ from the solution (3.25) we obtain

$$\langle e^{i\theta}\rangle_{\text{drifting}} = -\int_{-\pi}^{\pi}\int_{Kr}^{\infty}\rho(\theta',\omega)g(\omega)\mathrm{e}^{i\theta'}d\omega d\theta' + \int_{0}^{2\pi}\int_{Kr}^{\infty}\rho(\theta,\omega)g(\omega)e^{i\theta}d\omega d\theta \tag{3.34}$$

Noting the periodicity of the first term we can write:

$$\langle e^{i\theta}\rangle_{\text{drifting}} = -\int_{0}^{2\pi}\int_{Kr}^{\infty}\rho(\theta',\omega)g(\omega)e^{i\theta'}d\omega d\theta' + \int_{0}^{2\pi}\int_{Kr}^{\infty}\rho(\theta,\omega)g(\omega)e^{i\theta}d\omega d\theta \tag{3.35}$$

which finally leads to

$$\langle e^{i\theta}\rangle_{\text{drifting}} = 0 \tag{3.36}$$

This means that the drifting oscillators do not contribute to the order parameter.

Contribution of the *locked* oscillators to the order parameter

Now we consider the contribution of the locked oscillators. In the locked or synchronous state $|w| \leq Kr$, so we average over the unit circle for these frequencies

$$\langle e^{i\theta}\rangle_{\text{locked}} = \int_{0}^{2\pi}\int_{|\omega|\leq Kr}\rho(\theta,\omega)g(\omega)e^{i\theta}d\omega d\theta \tag{3.37}$$

From (3.20) we know that $\omega = Kr\sin(\theta)$, so that for each oscillator θ is fixed and depends on ω. That is:

$$\langle e^{i\theta}\rangle_{\text{locked}} = \int_{|\omega|\leq Kr} g(\omega)e^{i\theta(\omega)}d\omega \tag{3.38}$$

$$= \int_{-Kr}^{Kr} g(\omega)\cos(\theta(\omega) + i\sin(\theta(\omega)))d\omega \tag{3.39}$$

By assumption, $g(\omega)$ is symmetric around 0, and is an even function $g(-\omega) = -g(\omega)$, and consequently the imaginary part of (3.39) vanishes. Hence,

$$\langle e^{i\theta} \rangle_{\text{locked}} = \int_{-Kr}^{Kr} g(\omega) \cos(\theta(\omega)) d\omega \tag{3.40}$$

We can use (3.20) to change the variable of integration from ω to θ

$$\langle e^{i\theta} \rangle_{\text{locked}} = \int_{-\pi/2}^{\pi/2} g(Kr \sin(\theta)) \cos^2(\theta) d\theta \tag{3.41}$$

So finally, using (3.36) and (3.41), (3.28) can be written as:

$$r = \langle e^{i\theta} \rangle_{\text{locked}} + \langle e^{i\theta} \rangle_{\text{drifting}} \tag{3.42}$$

$$= Kr \int_{-\pi/2}^{\pi/2} g(Kr \sin(\theta)) \cos^2(\theta) d\theta \tag{3.43}$$

This is a *self-consistent* relation for r. Equation (3.43) always has a trivial solution, $r = 0$, for any value of the coupling constant K. This solution corresponds to the *incoherent state* (Fig. 3.2). Note also from (3.25), $\rho(\theta, \omega) = 1/2\pi$ for all values of θ and ω, meaning that there is an equal probability of finding an oscillator's phase anywhere on the circle.

For $0 < r \leq 1$ there corresponds another solution to (3.43) describing the *partially synchronised* state and is given by the solution of

$$1 = K \int_{-\pi/2}^{\pi/2} g(Kr \sin(\theta)) \cos^2(\theta) d\theta \tag{3.44}$$

This solution only exists for certain values of K and bifurcates from the $r = 0$ branch at some critical value K_c. To find this critical value, we let $r \to 0^+$ in (3.44) giving

$$1 = K_c \int_{-\pi/2}^{\pi/2} g(0) \cos^2(\theta) d\theta \tag{3.45}$$

$$= \frac{K_c g(0) \pi}{2} \tag{3.46}$$

and hence

$$K_c = \frac{2}{\pi g(0)} \tag{3.47}$$

This is the critical value that Kuramoto (1983) found for the onset of synchronisation.

It is interesting at this stage to see how the growth of r, at the critical point, scales with increasing K. To this end we can Taylor expand (3.44) around $r = 0$. We have for small r,

$$1 = K \int_{-\pi/2}^{\pi/2} \left[g(0) + g'(0) K r \sin(\theta) + \frac{1}{2} g''(0) K^2 r^2 \sin^2(\theta) \right] \cos^2(\theta)\ d\theta + \mathcal{O}(r^3) \tag{3.48}$$

Assuming that $g(\omega)$ is and even function with a maximum value at $\omega = 0$, we have $g'(0) = 0$, and so integrating (3.48) we have

$$1 = K \left[g(0) \frac{\pi}{2} + \frac{1}{16} \pi K^2 r^2 g''(0) \right] + \mathcal{O}(r^3) \tag{3.49}$$

$$= \frac{K}{K_c} + \frac{1}{16} \pi K^3 r^2 g''(0) + \mathcal{O}(r^3) \tag{3.50}$$

Noting $K \approx K_c$ near the critical point, we obtain

$$r \approx \frac{4}{K_c^2} \sqrt{-\frac{K - K_c}{\pi g''(0)}} \tag{3.51}$$

Therefore, near the critical point, the bifurcating branch scales as $(K - K_c)^{1/2}$. For the distributions of frequencies $g(\omega)$ we are interested in (Lorentzian and Gaussian for example), $g''(0) < 0$. However this may not be the case when we consider a uniform distribution of frequencies later on.

In order to obtain an explicit value for r, Kuramoto (1975, 1983) used a Lorentzian (or Cauchy) density for $g(\omega)$. The advantage with this choice of density is that it is possible to integrate (3.44) exactly.

The Lorentzian density is given by

$$g(\omega) = \frac{\gamma}{\pi(\gamma^2 + \omega^2)} \tag{3.52}$$

where γ is the distribution width. This is plotted and compared to the Gaussian density in Fig. 3.3.

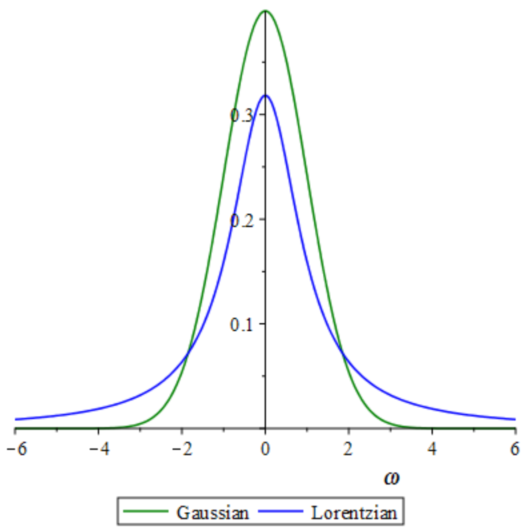

Figure 3.3: The Lorentzian distribution with $\gamma = 1$ and Gaussian distribution $\mathcal{N}(0,1)$, compared. The Lorentzian distribution has broader tails.

Substituting Eq.(3.52) into Eq.(3.44), we have

$$\begin{aligned} 1 &= K \int_{-\pi/2}^{\pi/2} g(Kr\sin(\theta))\cos^2(\theta)d\theta \\ &= \frac{K\gamma}{\pi} \int_{-\pi/2}^{\pi/2} \frac{1}{\gamma^2 + K^2r^2\sin^2(\theta)} \cos^2(\theta)d\theta \end{aligned} \tag{3.53}$$

Equation (3.53) can be integrated directly (using Maple) to give

$$1 = \frac{\gamma - \sqrt{K^2r^2 + \gamma^2}}{Kr^2} \tag{3.54}$$

Recognising that for the Lorentzian density, $K_c = 2/\pi g(0) = 2\gamma$, (3.54) can be solved for r leading to

$$r = \sqrt{1 - \frac{K_c}{K}} \tag{3.55}$$

Figure 3.4 shows the nature of this dependence.

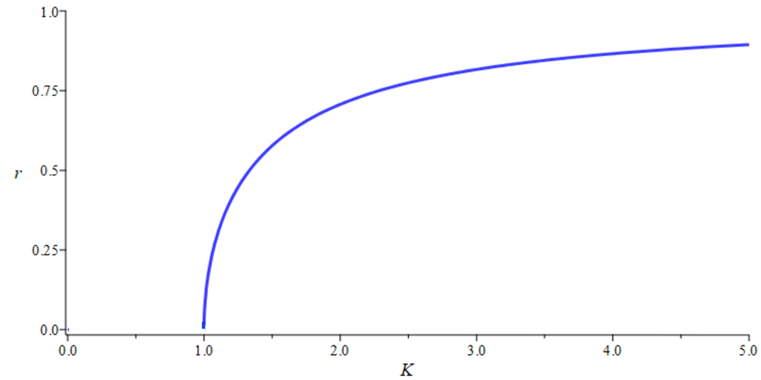

Figure 3.4: Order parameter r as a function of K given by (3.55) in the limit $N \to \infty$. Here $K_c = 1$. Partial synchronisation ($r > 0$) occurs when $K > 1$. When $K < 1$ there is no synchronisation and $r = 0$

3.4 Evolution of $r(t)$ and the Ott-Antonsen solution

Typical evolution of $r(t)$ is shown in Fig. 3.5 for $K > K_c$ (a) and $K < K_c$ (b), for a finite population. Various attempts have been made to derive an evolution equation for $r(t)$ for an infinite population. The first attempt was made by Kuramoto and

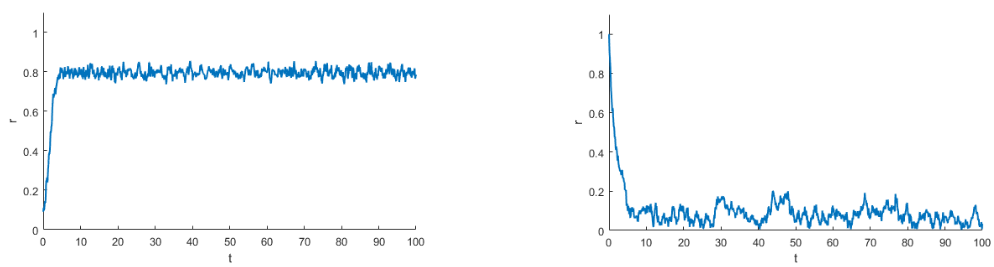

(a) (b)

Figure 3.5: Typical evolution of $r(t)$ from initially ordered (a) and disordered (b) states for a finite ($N = 200$) systems of oscillators.

Nishikawa (1987) who derived a fist order ordinary differential equation equation for $r(t)$ but made a series of invalid assumptions (Strogatz, 2000), one of which was to assume the drifting oscillators did not contribute to the evolution of r. Realising that drifting oscillators play a significant role in the evolution of r in the early transient stages they went on to derive, using intuitive and heuristic arguments, an integral equation for r (Kuramoto and Nishikawa, 1988). Watanabe and Strogatz (1993) derived a set of three couple differential equations and showed that $r(t)$ rises (or decays) exponentially as $K \geq K_c$ (or $K < K_c$) but only for oscillators with identical frequencies.

For a Lorentzian density of natural frequencies, Ott and Antonsen (2008, 2009) were able to determine an equation for the evolution of $r(t)$. The essence of the derivation is briefly outlined here. As $\rho(\theta, \omega, t)$ is 2π-periodic in t it may be expanded as a Fourier series

$$\rho(\theta, \omega, t) = \frac{1}{2\pi} \sum_{n=-\infty}^{\infty} \tilde{\rho}_n(\omega, t) e^{in\theta} \tag{3.56}$$

Ott and Antonsen introduce the ansatz

$$\tilde{\rho}_n = \alpha^n(\omega, t), \quad n \geq 0 \tag{3.57}$$

which replaces in infinite set of functions ρ_n by a single function, α. Further algebraic development (Gupta et al., 2014; Ott and Antonsen, 2008) leads to an expression for ρ,

$$\rho(\theta, \omega, t) = \frac{1}{2\pi} \frac{1 - |\alpha|^2}{(1 - |\alpha|)^2 + 4|\alpha| \sin^2(\theta - \phi)}, \tag{3.58}$$

where $\alpha(\omega, t) = |\alpha| e^{i\psi}$. Equation (3.58) can be directly compared to (3.25). In particular for $\alpha = 0$ the uniform distribution $\rho = 1/2\pi$ is obtained. As $\alpha \to 1$ a δ-distribution is obtained corresponding to locked oscillators.

Continued development using complex integration and the theory or residues (Gupta et al., 2014) leads finally to a first-order non-linear Ordinary differential equation for r

$$\dot{r}(t) + \left(\gamma - \frac{K}{2}\right) r(t) + \frac{K}{2} r^3(t) = 0 \tag{3.59}$$

equation (3.59) is easily integrated to give

$$r(t) = \begin{cases} r(0) \left| \dfrac{(K - 2\gamma)}{(K - 2\gamma - Kr^2(0))\mathrm{e}^{(2\gamma - K)t} + Kr^2(0)} \right|^{1/2}, & K \neq 2\gamma, \\ r(0) \left| 1 + 2\gamma r^2(0) t \right|^{-1/2}, & K = 2\gamma \end{cases} \tag{3.60}$$

Some example solutions to (3.60) are shown in Fig 3.6 for various values of $r(0)$.

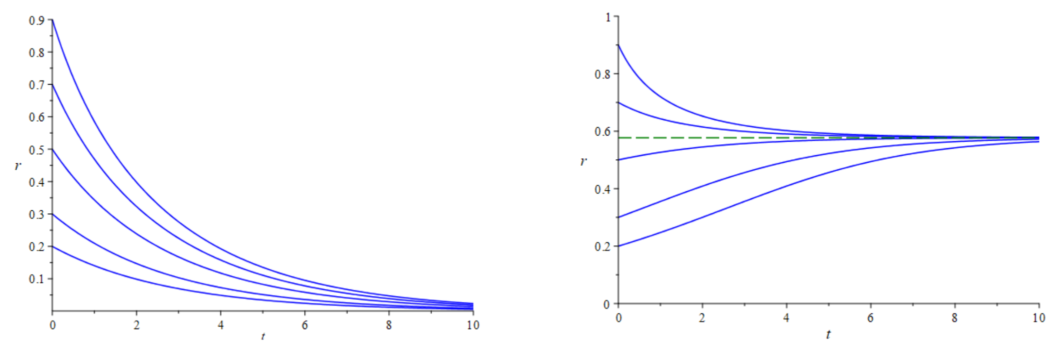

(a) $K = 0.3 < K_c$ (b) $K = 1.5 > K_c$

Figure 3.6: Solutions to the Ott-Antonsen equation for $r(t)$ with various starting conditions. A Lorentzian density with $\gamma = 1/2$ is used with critical coupling constant, $K_c = 1$. In the sub-critical region, the order parameter decays to zero for all starting values (a). In the super-critical region, the order parameter reaches a stable fixed point ($r = 0.577$ in this case) (b).

3.5 Linear stability analysis of the order parameter

At this stage is it worth exploring the linear stability of the fixed points of (3.59). Equation (3.59) can be written as

$$\dot{r}(t) = f(r) \tag{3.61}$$

where

$$f(r) = -\left(\gamma - \frac{K}{2}\right) r - \frac{K}{2} r^3 = 0 \tag{3.62}$$

From Eq. (3.62) we obtain the following fixed points:

$$r_1^* = 0 \tag{3.63}$$

$$r_2^* = \sqrt{1 - \frac{K_c}{K}} \tag{3.64}$$

In order to investigate the linear stability of the fixed points $r_{1,2}^*$ we compute $f'(r)$:

$$f'(r) = -\left(\gamma - \frac{K}{2}\right) - \frac{3K}{2} r^2 \tag{3.65}$$

and so, reaclling that $K_c = 2\gamma$

$$f'(r_1^*) = \frac{1}{2}(K - K_c) \tag{3.66}$$

$$f'(r_2^*) = -(K - K_c) \tag{3.67}$$

Hence the incoherent branch, is stable for $K < K_c$ and unstable for $K \geq K_c$. The second branch, or partially synchronised state, is stable as it exists only when $K > K_c$. The stability diagram is shown is in Fig.(3.7) and coincides with the behaviour seen in Fig.(3.6). It is clear that r undergoes a *supercritical pitchfork bifurcation* at $K = K_c$. This may be expected from (3.59), as with suitable rescaling it corresponds to the normal form for a supercritical pitchfork bifurcation.

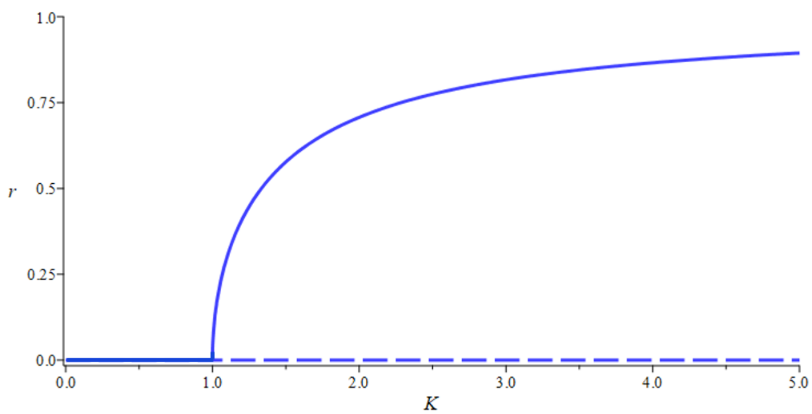

Figure 3.7: Supercritical pitchfork bifurcation of r. In this example the critical coupling $K_c = 1$. For $K < K_c$ the only solution is $r = 0$. For $K > K_c$ there are two branches; $r = 0$ and $r = \sqrt{1 - K_c/K}$. Numerical simulation (see Chapter (4)) suggests that the $r = 0$ branch becomes unstable for $K > K_c$ whereas the $r = \sqrt{1 - K_c/K}$ branch is stable.

Returning to the solution given in (3.60) it is interesting to examine the asymptotic behaviour as $t \to \infty$. If $K < 2\gamma = K_c$, it is straightforward to see from (3.60) that $\lim_{t\to\infty} r(t) = 0$. If $K > 2\gamma = K_c$ then $\lim_{t\to\infty} r(t) = \sqrt{1 - \frac{K}{K_c}}$ if $r(0) > 0$, and $\lim_{t\to\infty} r(t) = 0$, if $r(0) = 0$.

All of the above analysis take place in the continuum (or thermodynamic) limit, $N \to \infty$.

3.6 Gradient system and Lyapounov function

Here we show that the globally coupled Kuramoto model (3.1) forms a gradient system where the function

$$V(\theta) = -\sum_{j=1}^{N} \omega_j \theta_j - \frac{K}{N} \sum_{i}^{N} \sum_{j>i}^{N} \cos(\theta_j - \theta_i) \tag{3.68}$$

is a potential function (Ha et al., 2013; van Hemmen and Wreszinski, 1993). It is easy to see this is so by differentiating V

$$\frac{\partial V}{\partial \theta_i} = -\omega_i - \frac{K}{N} \sum_{j=1}^{N} \sin(\theta_j - \theta_i), \quad i = 1, \ldots N, \tag{3.69}$$

Hence

$$\dot{\theta}_i = -\frac{\partial V}{\partial \theta_i}, \quad i = 1, \ldots N, \tag{3.70}$$

and so (3.1) is a gradient system

$$\dot{\boldsymbol{\theta}} = -\boldsymbol{\nabla}(V) \tag{3.71}$$

It is possible for the globally coupled Kuramoto model to use the normalised scalar potential V as a measure of synchrony. In this case $V = 1$ corresponds to complete disorder and $V = 0$ to complete synchronisation. Differentiating $V(\theta)$ w.r.t. time

$$\dot{V} = \sum_{i=1}^{N} \frac{\partial V}{\partial \theta_i} \frac{\mathrm{d}\theta}{\mathrm{d}t} \tag{3.72}$$

$$= -\sum_{i=1}^{N} \left(\frac{\partial V}{\partial \theta_i} \right)^2 \tag{3.73}$$

$$= -\|\boldsymbol{\nabla}(V)\|^2 \leq 0 \tag{3.74}$$

where $\| \cdot \|$ is the usual vector norm.

So V is also a Lyapounov function. This means all trajectories of (3.1) flow 'downhill' on the potential surface of V to its minima (if one exists) and reaches the fixed points asymptotically. It is not possible for other outcomes such as such as limit cycles or strange attractors.

Chapter 4

Numerical simulation of the globally coupled Kuramoto model

4.1 Distribution of identical oscillator frequencies

The analysis of previous chapters has been within the framework of an infinite number of oscillators. Only by moving to the $N \to \infty$ limit was it possible to obtain any analytical results concerning the transition to synchronisation of a population of couple oscillators. Now we return to the finite-N formulation and explore the behaviour of the globally coupled Kuramoto model (3.1) through numerical simulation.

First we consider the evolution of population of 100 oscillators with a distribution of identical natural frequencies, $g(\omega) = \delta(\omega)$. Here the phases of each oscillator are initially placed randomly on the unit circle, so starting in a disordered state. The system of ordinary differential equations (3.1) is integrated for 100 time units. Figure 4.1(a) show the initial distribution of phases for a typical simulation run. The initial magnitude of r, is very small in this state as indicated by the blue arrow. After a very short length of time (approximately $t = 10$) the phases of all oscillators have converged onto a common value of just greater than 1 where they remain indefinitely as shown if Fig.4.1(c). All oscillators now have the same phase and they are fully synchronised. Figure 4.1(b) shows the end state of for the phases. Figure 4.1(c) shows that that the synchronisation of phases occurs as soon as the simulation starts and reaches perfect synchronisation very quickly. The magnitude of the order parameter r rises very quickly from a disordered value to perfect synchronisation $r = 1$. This spontaneous synchronisation occurs for any value of the coupling constant K. The critical coupling constant in this case is $K_c = 0$ (Gherardini et al., 2018).

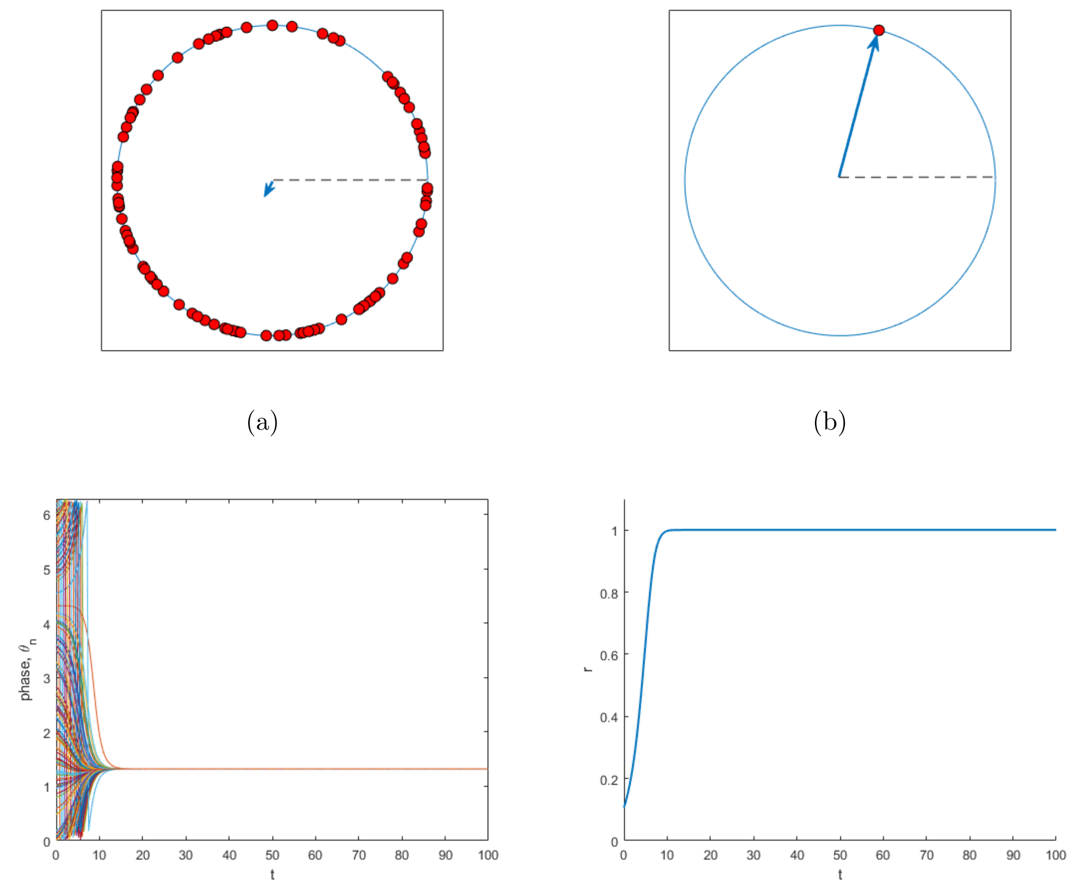

(a) (b) (c) (d)

Figure 4.1: Spontaneous synchronisation of $N = 100$ oscillators with identical natural frequencies. Here the coupling constant $K = 0.8$. Starting from an initially incoherent state with oscillator phases distributed randomly on the circle (a), phases rapidly converge onto a single value (c) finally reaching complete synchronisation after a short time (b). The evolution of r shows this rapid transition to complete synchronisation (d)

4.2 Unimodal distribution of oscillator frequency (Lorentzian density).

4.2.1 Subcritical coupling

For identical oscillators we have seen that complete synchronisation occurs for any initial condition as the critical coupling (K_c)is effectively zero. We now turn our attention to exploring the dynamics when the distribution of intrinsic oscillator frequencies are drawn from a unimodal density such as a Gaussian or Lorentzian density. The aim here is to explore each region of the stability diagram Fig. 3.7 for finite N. We consider a population of 250 oscillators with natural frequencies drawn from a Lorentzian distribution with $\gamma = 1/2$.

We start in the subcritical region ($K < K_c$) with an initially fully synchronised state ($r = 1$) indicated by the red point in Fig.4.2 (a). Every oscillator is started with the same phase (completely synchronised). Fig.4.2 (b) shows the evolution of $r(t)$ and is compared to the theoretical value obtained from the Ott-Antonsen equation (3.59). It is clear the initial coherent state is unstable in this region and quickly converges onto a stable incoherent state ($r = 0$). Oscillations in r are due to the finite size of the population and are of order $N^{-1/2}$. Fig. 4.2(c) shows the phase of each oscillator at the end of the integration period where oscillators are ordered by natural frequency (index-n). Fig.4.2(d) shows the angular velocity $\Omega = \dot{\theta}$ averaged over a short interval near the end of the integration time. No synchronisation is visible and the oscillator phases are scattered with variation in angular speeds. The angular speeds Ω_i are symmetrical around the mean angular speed ($\Omega = \langle\omega\rangle = 0$). Fast and slow oscillators can be seen at low and high values of natural frequency (index-n).

In Fig. 4.3 the initial condition is the completely disordered or splay state ($r = 0$). Oscillator phases are initially distributed evenly around the unit circle, as far as is possible within the confines of computer roundoff error. Aside from finite N fluctuations, the oscillators maintain their incoherence in phase, and after numerous similar integrations in this part of the stability diagram we can conclude that this branch is stable.

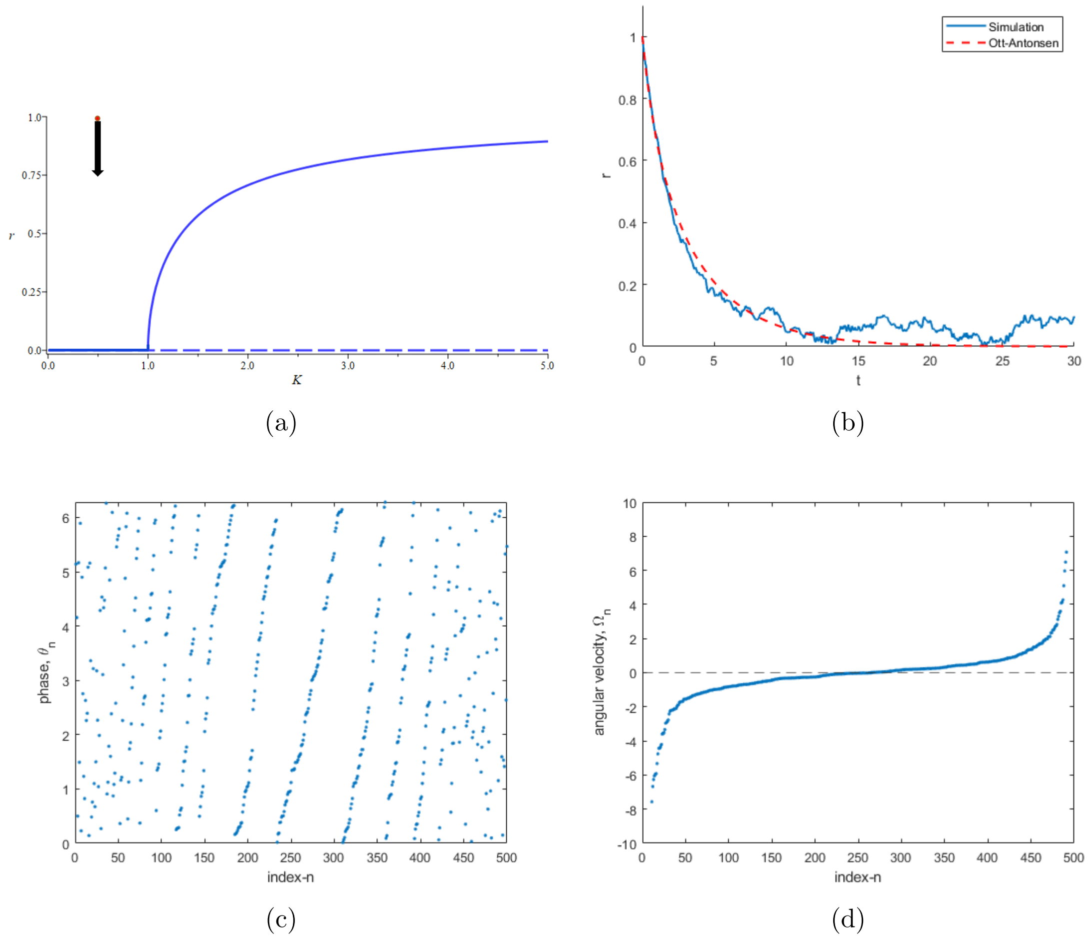

Figure 4.2: Dynamics of $N = 500$ oscillators with subcritical coupling ($K = 0.5$, with $K_c = 1$) with natural frequencies drawn from a Lorenztian distribution (3.52) with $\gamma = 1/2$. Oscillators are initially in a completely coherent state $r = 1$ (red point). Evolution evolves rapidly towards the incoherent state with the r decaying to zero and following the Ott-Antonsen solution (3.60) closely apart from fluctuations (b). The oscillator phases, ordered by natural frequency (index-n), are randomly distributed (c) and the angular speeds Ω_i all vary around the mean $\Omega = 0$ with fast and slow oscillators in the tails. There is some structure appearing in the distribution of phases (c) and in this instance is due to the non zero value of r during the final stages of integration.

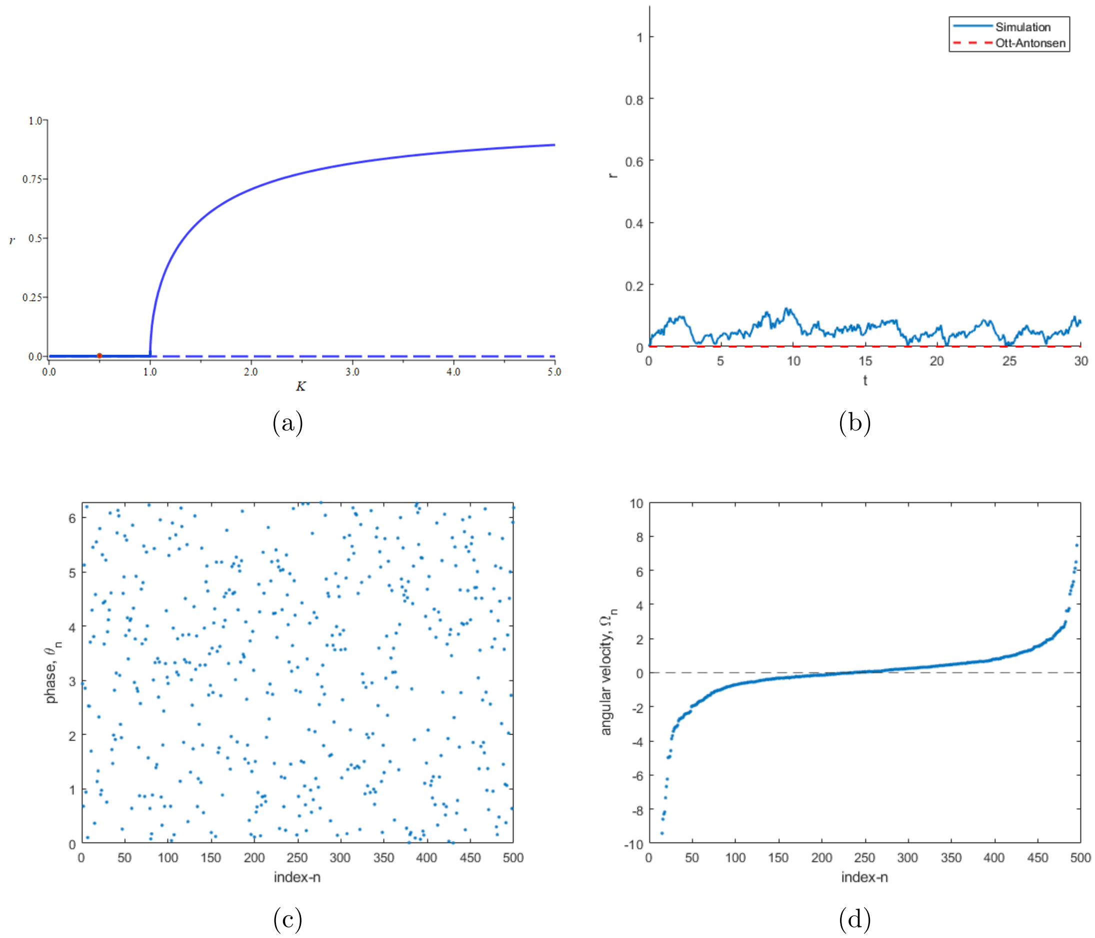

Figure 4.3: Dynamics of $N = 500$ oscillators with subcritical coupling ($K = 0.5$, with $K_c = 1$) with natural frequencies drawn from a Lorenztian distribution (3.52) with $\gamma = 1/2$. Oscillators are initially in a completely incoherent state $r = 0$ (red point). The oscillators remain in the incoherent state with the r remaining around zero and following the Ott-Antonsen solution (3.60) closely apart from fluctuations (b). The oscillator phases, ordered by natural frequency (index-n), are randomly distributed (c) and the angular speeds Ω_i all vary around the mean $\Omega = 0$ with fast and slow oscillators in the tails.

4.2.2 Supercritical coupling

Next we consider the case where the coupling is supercritical ($K > K_c$). Three regions of the stability diagram are explored.

Firstly we consider starting in an initial completely synchronised state with $K = 2.0 > K_c$. Figure 4.4 shows the results from a typical integration in this regime. The initial perfect coherence ($r = 1$) reduces rapidly to the theoretically predicted value of $\sqrt{1 - K_c/K} \approx 0.71$ as shown in Fig.4.4 (b) and the evolution of r follows the Ott-Antonsen solution closely. This is a state of partial synchronisation and is seen clearly in Fig.4.4 (c) where oscillators near to the central frequency are synchronised with non-synchronised or drifting oscillators visible in the tails. The angular speed Ω_i of these synchronised oscillators are identical (and equal to zero in the rotating frame) as shown in Fig.4.4 (d). So we have a synchronised group around the central frequency together with fast and slow drifters at either end of the natural frequency distribution.

Next we start in an incoherent state where $r \gtrsim 0$ as shown in Fig. 4.5(a). As before r converges rapidly to the theoretical value (0.71) but this time from below resulting in a partially synchronised state.

In order to explore the stability of the branch ($r = 0$, $K > K_c$) we start as close as possible to $r = 0$ (Fig. 4.6). In this state initial phases are distributed evenly around the circle giving an initial $r = 0$. Again r rises rapidly to its predicted value leading to a partially synchronised state. The initial distribution of phases leads to a value of r that is very close to zero but not exactly so due to computer roundoff error. This acts as a very small perturbation about the fixed point $r = 0$ and suggests that this branch is unstable.

Numerous integrations were carried out with similar parameters leading to similar results.

In summary we have explored all regions of the stability diagram (Fig. 3.7) and have confirmed numerically the stability properties of each branch. We have also shown that r undergoes a supercritical pitchfork bifurcation at $K = K_c$.

Finally we investigate the form of a potential phase transition from incoherent to coherent states as K is varied. To this end we perform fifty separate integrations with $N = 500$ oscillators with natural frequencies drawn from a Lorentzian distribution with $\gamma = 1/2$. The final value of r for each value of K is obtained by averaging the fluctuating value of r over the final 10% of time so that transients have disappeared. Figure 4.7 shows the results of these integrations showing clearly a second-order, or continuous, phase transition at the critical coupling.

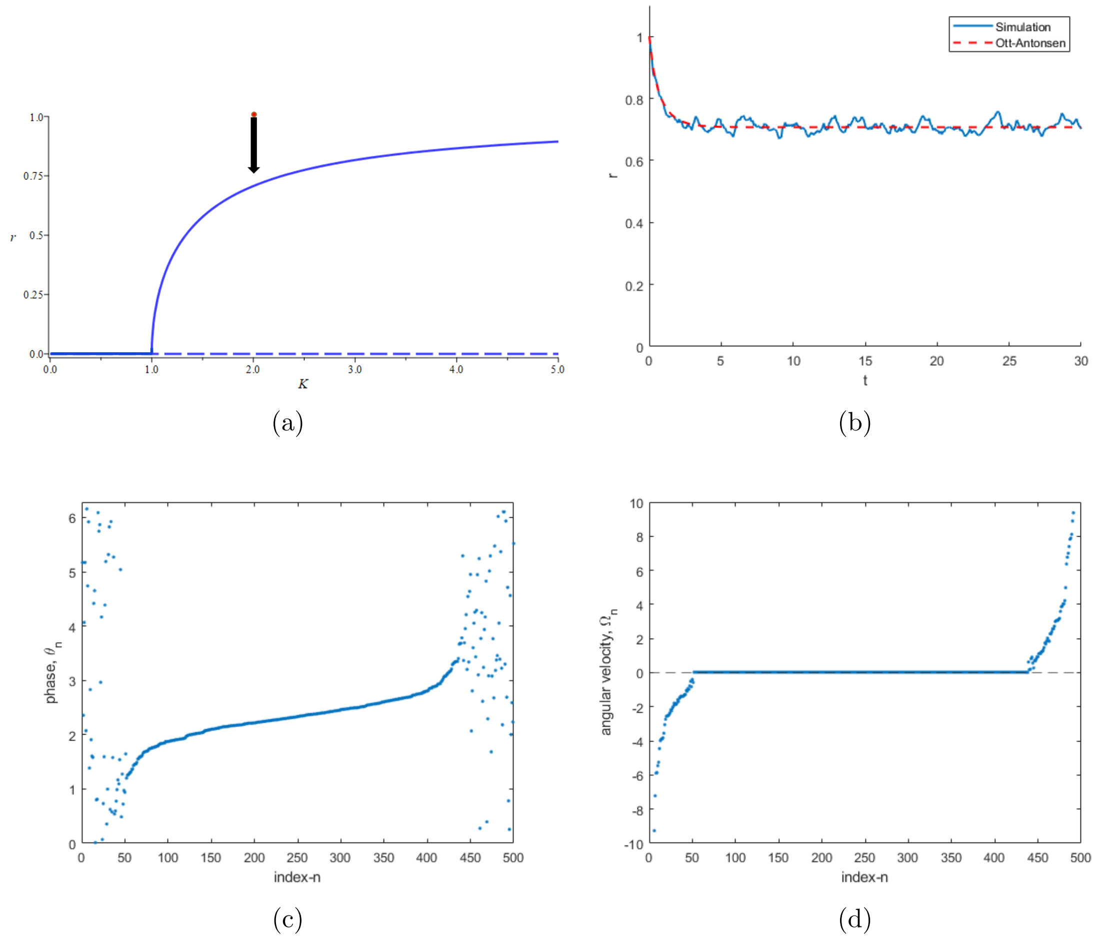

Figure 4.4: Dynamics of $N = 500$ oscillators with supercritical coupling ($K = 0.5$, with $K_c = 1$) with natural frequencies drawn from a Lorenztian distribution (3.52) with $\gamma = 1/2$. Oscillators are initially in a completely coherent state $r = 1$ (red point). r reduces rapidly to the theoretically predicted value of $\sqrt{1 - K_c/K} \approx 0.71$ and follows the Ott-Antonsen solution (3.60) (in red) closely apart from fluctuations (b). The oscillator phases, ordered by natural frequency (index-n), show partial synchronisation where oscillators near to the central frequency are synchronised (c) and the angular speeds Ω_i of these synchronised oscillators are identical (and equal to zero in the rotating frame) with fast and slow drifting oscillators in the tails.

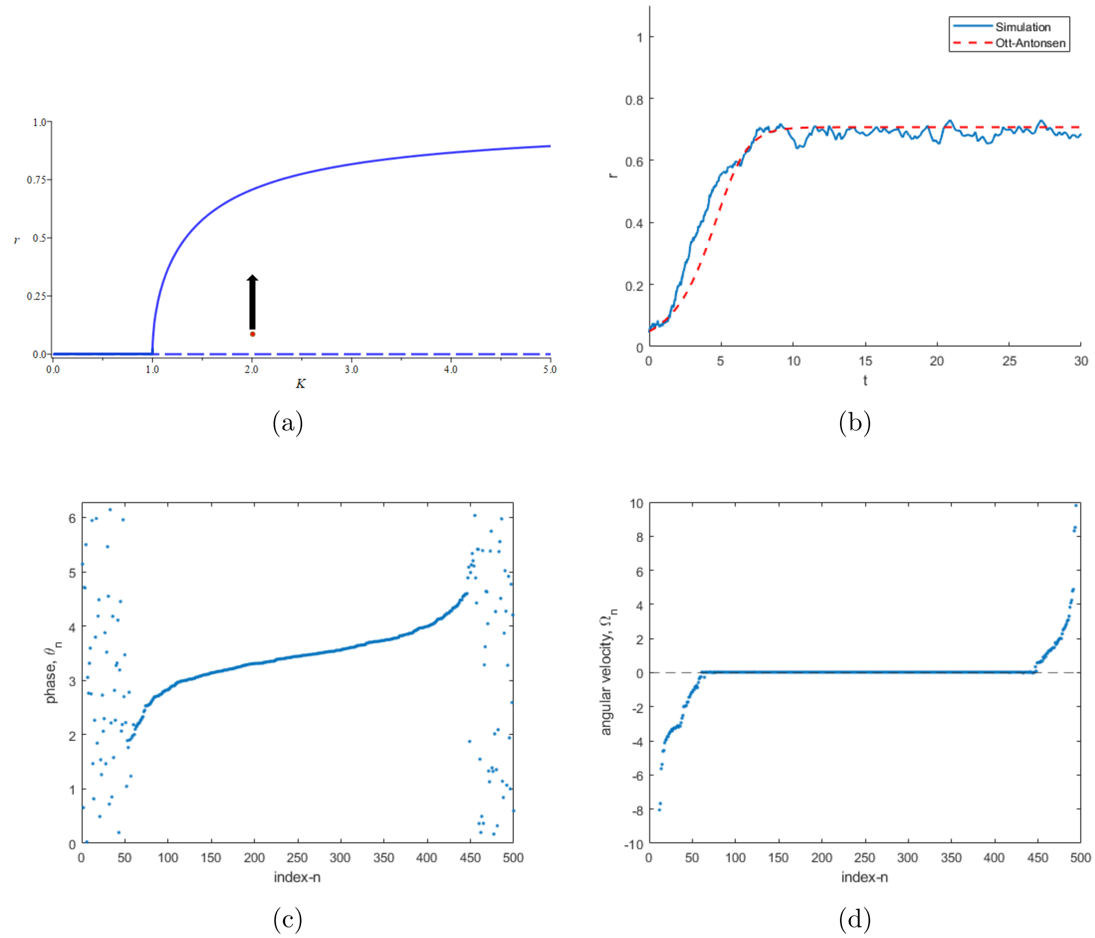

Figure 4.5: Dynamics of $N = 500$ oscillators with supercritical coupling ($K = 0.5$, with $K_c = 1$) with natural frequencies drawn from a Lorenztian distribution (3.52) with $\gamma = 1/2$. Oscillators are initially in a *incoherent* state $r \gtrsim 0$ (red point). r increases rapidly to the theoretically predicted value of $\sqrt{1 - K_c/K} \approx 0.71$ and follows the Ott-Antonsen solution (3.60) (in red) closely apart from fluctuations (b). The oscillator phases, ordered by natural frequency (index-n), show partial synchronisation where oscillators near to the central frequency are synchronised (c) and the angular speeds Ω_i of these synchronised oscillators are identical (and equal to zero in the rotating frame) with fast and slow drifting oscillators in the tails.

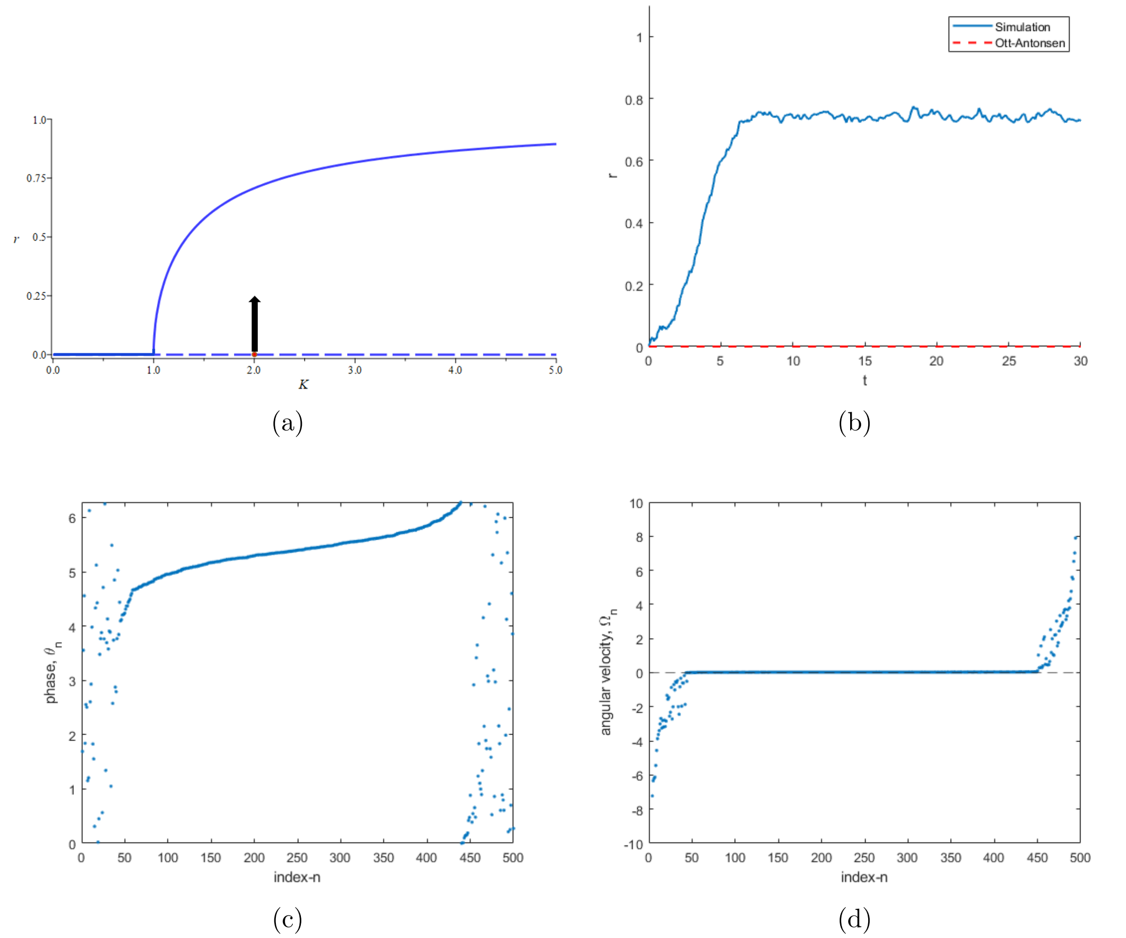

Figure 4.6: Dynamics of $N = 500$ oscillators with supercritical coupling ($K = 0.5$, with $K_c = 1$) with natural frequencies drawn from a Lorenztian distribution (3.52) with $\gamma = 1/2$. Oscillators are initially in a *completely incoherent* or *splay* state $r = 0$ (red point). r increases rapidly to the theoretically predicted value of $\sqrt{1 - K_c/K} \approx 0.71$ but does not follow the Ott-Antonsen solution (3.60) (in red) suggesting that this branch is unstable to small perturbations (b). The perturbation is provided by computer roundoff error. The oscillator phases, ordered by natural frequency (index-n), show partial synchronisation where oscillators near to the central frequency are synchronised (c) and the angular speeds Ω_i of these synchronised oscillators are identical (and equal to zero in the rotating frame) with fast and slow drifting oscillators in the tails.

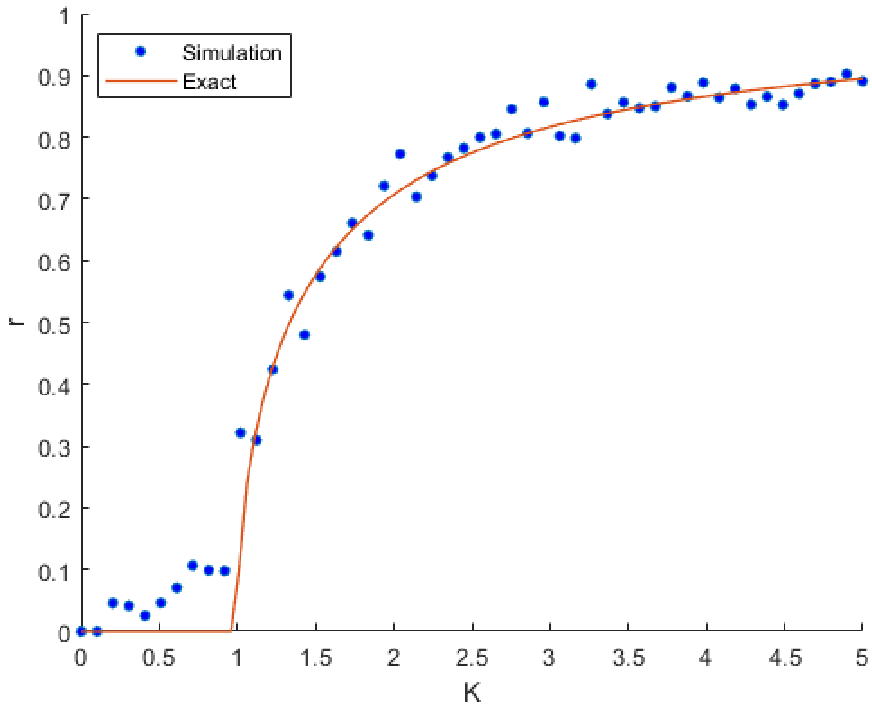

Figure 4.7: Synchronisation of $N = 500$ oscillators with natural frequencies drawn from a Lorentzian distribution (3.52) and random initial phases. A second-order phase transition occurs at $K_c = 1$ with a continuous transition from disordered to ordered state. Values of r are obtained by averaging over a time period (the last 10%) after transients have decayed and a stationary state is reached. The red curve shows the exact dependence of r on K showing the $(K - K_c)^{1/2}$ scaling near the critical point.

4.3 Uniform distribution of oscillators and explosive synchronisation

We have seen that for a Unimodal and symmetrical distribution of natural frequencies (Lorentzian for example) we obtain a second-order phase transition at the critical coupling value K_c. In this case we used the fact that $g''(0) < 0$ in order to derive the behaviour of r near to the phase-transition. Pazó (2005) considered the case of uniformly distributed frequencies and found that at the critical frequency, r changes discontinuously from zero to $r_c = \pi/4$ and is a *first-order* phase transition. This is an example of *explosive synchronisation*. Further increase in coupling strength K leads to increase in r towards one. Pazo also went on to show that near to this critical value r scales like, $r \sim \pi/4 + (K - K_c)^{2/3}$ in contrast to the $r \sim (K - K_c)^{1/2}$ scaling for a unimodal distribution.

Here we consider a Uniform distribution of natural frequencies,

$$g(\omega) = \begin{cases} \dfrac{1}{2\gamma}, & |\omega| \leq \gamma, \\ 0, & |\omega| > \gamma \end{cases} \tag{4.1}$$

We chose a supercritical coupling constant $r = 0.8$ and take $\gamma = 1/2$, which leads to a critical coupling constant of $K_c = 2/\pi$ and integrate $N = 500$ oscillators over a time of $t = 100$. Figure 4.8(a) shows how the oscillator's initially random phases *all* become entrained at around $t = 20$ with Figure 4.8(b) showing the corresponding rapid rise in r.

Figure 4.9 shows the results of 50 separate integrations with $N = 1000$ and with K varying between 0 and 1.5. Each oscillator has a natural frequency drawn from a Uniform distribution (4.1) and initial phases randomly assigned on the circle. The transition from the disordered to ordered state through a first-order phase transition at the critical value $K_c = 2/\pi$ is seen. r rises abruptly to $\pi/4$ at the critical value and the $(K - K_c)^{2/3}$ scaling when $K > K_c$ can be seen.

4.4 Introducing a phase shift - the Kuramoto-Sakaguchi model

So far we have considered the simplest form for the interaction of phases, namely $\sin(\theta_j - \theta_i)$. If $\theta_j > \theta_i$ the the phase of oscillator i will accelerate $\dot{\theta} > 0$. If $\theta_j < \theta_i$ the the phase of oscillator i will decelerate $\dot{\theta} < 0$. For a unimodal distribution of natural frequencies we have seen this can lead to drifting and locked oscillators and for identical oscillators (delta function distribution of natural frequencies) this leads to all oscillators synchronising.

Sakaguchi and Kuramoto (1986) modified this basic model by introducing a constant phase shift α to the coupling function through the model

$$\dot{\theta}_i(t) = \omega_i + \frac{K}{N} \sum_{j=1}^{N} \sin(\theta_j(t) - \theta_i(t) + \alpha), \quad |\alpha| \leq \pi/2 \tag{4.2}$$

Here the coupling function does not vanish when phases align and α acts to *frustrate* the attempt to synchronise. For $\alpha \neq 0$, the contribution made by the interaction function does not vanish for in-phase alignment, which effectively impedes synchronization. Here we briefly investigate the effect of the additional parameter α on the synchronisation of oscillators with distributed natural frequencies.

Figure 4.10 shows the variation of r with the coupling strength K for different values of the *frustration parameter* α. Thirty separate integrations were carried out for each value of $\alpha = 0, \pi/4, \pi/3$. $N = 1000$ oscillators were used with natural frequencies drawn from a Lorentzian distribution (with $\gamma = 1/2$) and were initially distributed randomly on the circle.

It is clear that increasing the value of α impedes the process of synchronisation by increasing the critical coupling parameter K_c with increasing α.

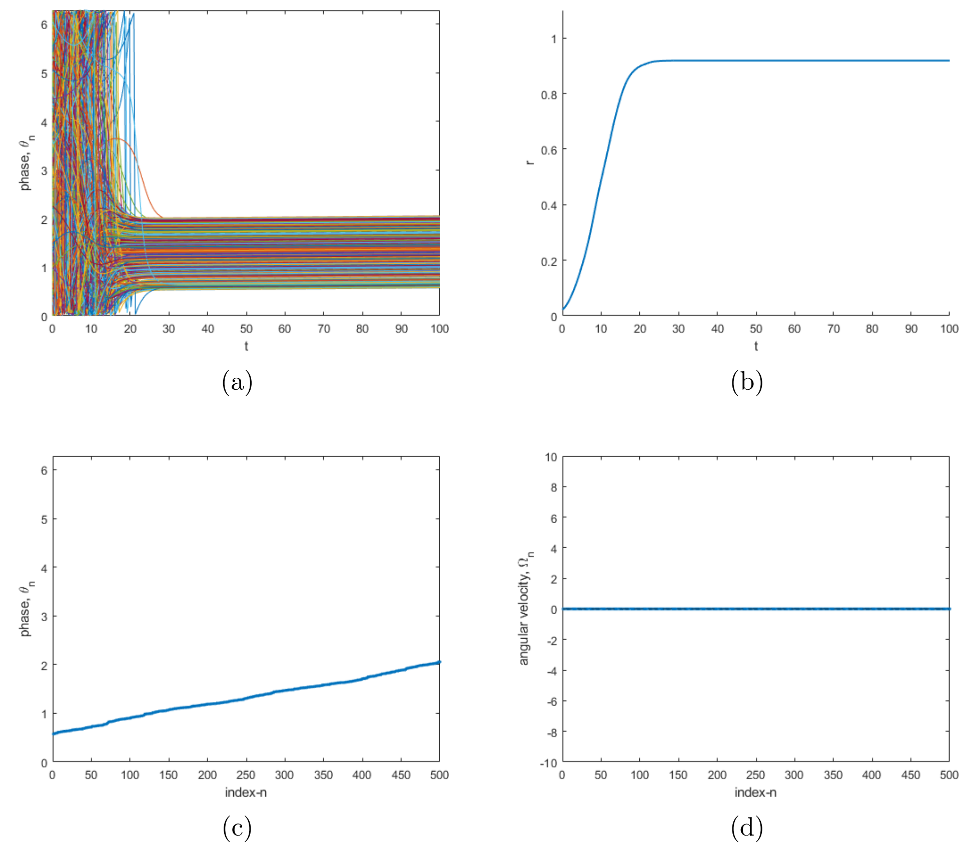

Figure 4.8: Evolution of $N = 500$ oscillators with natural frequencies drawn from a Uniform distribution from an initially incoherent start. The coupling is supercritical ($K = 0.8 > K_c$). The phase rapidly align around a mean phase into a coherent synchronised state (a) also shown by the rapid increase in r (b). Note that *all* oscillators end up in the synchronous group. The oscillator phases, ordered by natural frequency (index-n), show full synchronisation (c) and the angular speeds Ω_i of these synchronised oscillators are identical (and equal to zero in the rotating frame) with no drifting oscillators in the tails.

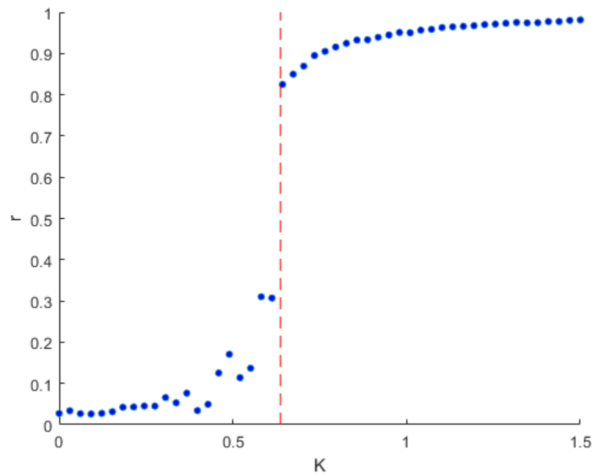

Figure 4.9: Explosive synchronisation of $N = 1000$ oscillators with natural frequencies drawn from a Uniform distribution (4.1) and random initial phases. A first-order phase transition occurs at $K_c = 2/\pi$. Values of r are obtained by averaging over a time period (the last 10%) after transients have decayed and a stationary state is reached. The $(K - K_c)^{2/3}$ (for $K > K_c$) scaling near the critical point can be seen.

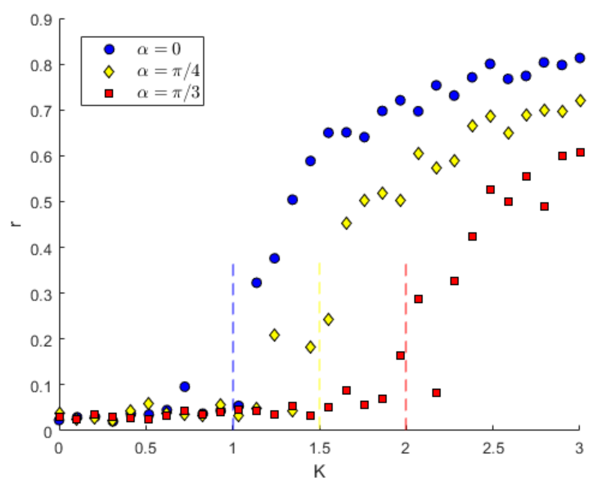

Figure 4.10: Delay to the phase-transition to synchronisation due to the inclusion of a phase-shift or *frustration* parameter into the coupling function. Here $N = 1000$ oscillators with natural frequencies drawn from a Lorenztian distribution (with $\gamma = 1/2$) are modelled using (4.2) with three values for α. Initial phases were randomly distributed on the circle (disordered state). It is clear that as α is increased the phase transition occurs at larger critical values of K.

Chapter 5

Chimera states on a non-locally coupled 1D ring network

5.1 Kuramoto-Sakaguchi model on a network topology

The models considered in previous chapters have centred around a population of oscillators where each oscillator is coupled to every other oscillator in a global all-to-all coupling. In the language or network theory, the oscillators reside at the nodes of a *complete network* (or graph). Oscillators evolve either into incoherent, synchronised or partially synchronised states.

Many authors have considered the situation where oscillators reside at the nodes of other network topologies. The simplest case is a one-dimensional line or ring network (Abrams and Strogatz, 2004, 2006; Kuramoto and Battogtokh, 2002; Laing, 2009) which can easily be extended to a two-dimensional array of oscillators (Kim et al., 2004; Martens et al., 2010; Shima and Kuramoto, 2004). A large amount of research has also been carried out into synchronisation of Kuromoto-type models on complex networks (Rodrigues et al., 2016). A further modification can also be made to the complete all-to-all coupled network if the coupling is assumed to be inhomogeneous (Ko and Ermentrout, 2008) or the newtork consists of two sub-populations with couple within and between them (Abrams et al., 2008).

In all of these situations new rich and exciting behaviour can be seen.

5.2 Coexistence of coherence and incoherence

Next we consider the Kramoto-Sakaguchi model on a one-dimensional ring network with non-local coupling. Kuramoto and Battogtokh (2002) considered this case for identical oscillators. Their model in the continuum limit was

$$\frac{\partial}{\partial t}\theta(x,t) = \omega - \int_0^1 G(x-x')\sin\left(\theta(x,t) - \theta(x',t) + \alpha)\right)dx' \tag{5.1}$$

where

$$G(x-x') = \frac{\kappa}{2}e^{(-\kappa|x-x'|)} \tag{5.2}$$

which is a reduced phase description derived from a complex Ginzburg-Landau equation with weak coupling. The space variable $x \in [0,1]$ is a periodic variable and can be interpreted as an angle on a circle (mod 1) (Abrams and Strogatz, 2006). Non-local coupling is provided by the kernel function $G(x-x')$ and decreases with oscillator separation.

Numerical exploration of a discrete version of (5.1) with particular values for α and κ and certain initial conditions, they found the system evolves to a coherent synchronised state co-existing with incoherent drifting oscillators. This was completely unexpected as all oscillators were identical and symmetrically coupled with each other.

Abrams and Strogatz (2006) named these states "*chimera states*" where coherence and incoherence exist at the same time. It is not obvious that the oscillators would evolve into anything but the fully synchronous state, and yet chimeras are regularly observed. These states cannot form in globally coupled or locally coupled systems. If $G(x) \equiv 1$, then a Lyapounov function exists and all states converge on the synchronous states as outlined in section 3.6. If $\alpha = 0$, for any value of $G(x)$, then (5.1) is a gradient system and evolves towards a fixed-point of the synchronous state (Abrams and Strogatz, 2006) (see section 3.6). Hence coherence and incoherence cannot exist together in these circumstances.

In order to describe the degree of synchrony in the current situation, the global order parameter defined by (3.6) is no longer suitable, and a complex spatial order parameter is introduced (Kuramoto and Battogtokh, 2002).

$$R(x,t)e^{i\psi_j(x,t)} = \int_0^1 G(x-x')e^{\theta(x',t)}dx' \tag{5.3}$$

This spatial order parameter provides a measure of *local coherence* on the ring.

Fig. 5.1 shows results from numerical integration of (5.1) with $N = 512$ oscillators. The chimera can be seen in Fig. 5.1(a), where phase coherence can be seen near the boundary ($x \approx 0$ and $x \approx 1$) and incoherence where $0.2 < x < 0.8$. The corresponding value of $R(x)$ for this state is shown in Fig. 5.1,(b).

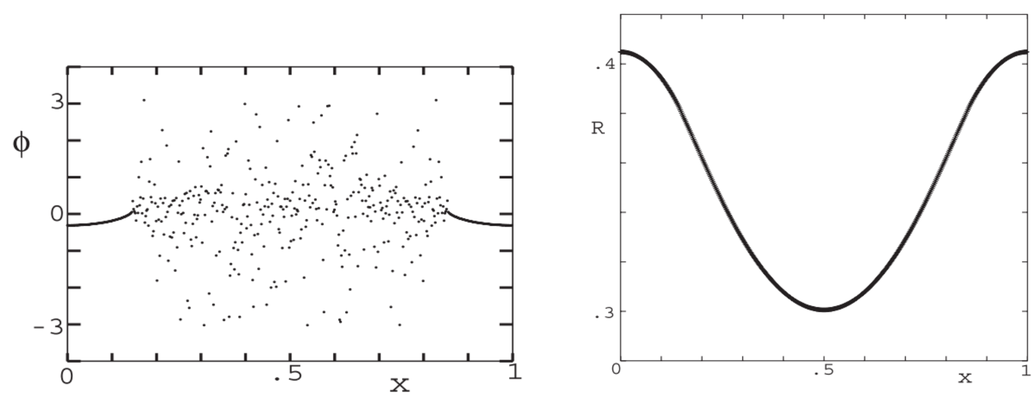

(a) (b)

Figure 5.1: Taken from Kuramoto and Battogtokh (2002), a snapshot of the distribution of phases obtained from (5.1) with $N = 512$, $\alpha = 1.457$, $\kappa = 4.0$ (a), together with the amplitude of spatial order parameter $R(x)$ (b).

5.3 Numerical simulation

To explore the occurrence of chimera states numerically we consider a Kuramoto-Sakaguchi model with non-local coupling on a one-dimensional ring. We consider N identical oscillators placed evenly around the ring and modelled by

$$\dot{\theta}_i(t) = \omega + \frac{2\pi}{N}\sum_{j=1}^{N} G\left(\frac{2\pi|i-j|}{N}\right)\sin(\theta_j(t) - \theta_i(t) + \alpha) \quad i = 1, \dots N \tag{5.4}$$

with coupling provided by the kernel

$$G(x) = \frac{1}{2\pi}\left(1 + A\cos x\right) \tag{5.5}$$

where, $0 \leq A \leq 1$, gives a measure of how far the non-local coupling varies from global coupling.

The relevant spatially discrete version of $R(x,t)$ is given by (Laing, 2009)

$$R_i(t)e^{i\psi_j(x,t)} = \frac{2\pi}{N}\sum_{j=1}^{N} G\left(\frac{2\pi|i-j|}{N}\right)e^{i\theta_j(t)} \tag{5.6}$$

Numerous simulations are run with a variety of values for the 'tunable' parameters A and α as well as a varying initial conditions. A variety of final states were observed. Sometimes complete disorder with drifting oscillators. Other times complete synchronisation of all oscillators, and occasionally chimera states. It is clear that there is a sensitive dependence of the relative values of these parameters to the corresponding final state. Often there is a dynamical evolution from one state to another over time.

Figure 5.2 shows the output from a typical integration of (5.1). Here we choose $\alpha = 1.37$, $A = 0.95$, $N = 250$ and we start from an initially disordered state and integrate for $t = 200$. A chimera can easily be seem in Fig. 5.2(a) where phase coherence can be seen at locations $125 \lesssim n \lesssim 245$ on the ring and incoherence and drifting oscillators elsewhere. The corresponding $R(x)$ can be seen in Fig. 5.2(b) and areas of coherence correspond to higher values of $R(x)$. Another way to visualise the chimera state is to wrap the phase space (x, θ) on a torus. Figure 5.3 shows the phase pattern displayed in Fig. (5.2) on a torus where the azimuthal angle represents position on the ring x and latitude represents phase of each oscillator, $\theta(x)$ at that location. The coherent and incoherent oscillators can easily be seen.

Figures 5.2 and 5.3 display a 'snapshot' of $\theta(x)$ and $R(x)$ at a single value of time, but it will be interesting to see the evolution of the phases across the entire integration time $t = 0 \ldots 200$.

Figure 5.4(a) shows the phase $\theta(x)$ of each oscillator at its location on the ring (given here by the index n) over time. Starting from an initial disordered state it is possible to see coherent phases at locations $125 \lesssim n \lesssim 245$ on the ring and

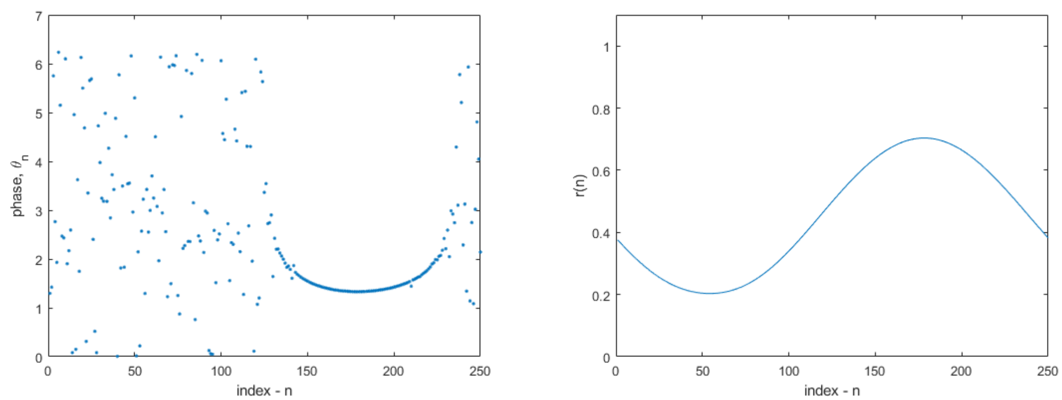

(a) (b)

Figure 5.2: Snap shot of a typical chimera obtained from the system 5.4. (a) shows the phase of each oscillator at each location on the ring (index-n and (b) shows the $R(x)$, the magnitude of the spatial order parameter at around the ring. Here $N = 250$, $\alpha = 1.37$, $A = 0.95$.

incoherence and drifting oscillators elsewhere. However $R(x,t)$ gives a clearer picture of the evolution of the chimera over this timescale. Figure 5.4(b) shows the evolution of $R(x,t)$, the amplitude of the spatial order parameter. Staring from an initially disordered state (in blue) a chimera emerges after about $t \approx 7$ and continues to exist throughout the integration time. However, the coherent and incoherent regions do not remain static over time. The spatial extent of the coherent oscillators varies as can be seen in oscillations of R over time.

In the single case considered here, the chimera state seems to be stable over the limited integration time ($t = 200$). However from other integrations using the same parameters this is not always the case. The only variation in each integration is the randomness introduced into the initial conditions (the initial distribution of phases on the ring).

In order to explore this further numerous additional integrations were carried out using the identical values of the parameters α and A all staring from a random disordered state.

Figure 5.5 shows the results from four typical integrations with the same parameters but over a time of $t = 1000$. In each case the initial state is one of disorder (blue) but with different randomisation of initial phases on the circle.

In Figure 5.5(a) the initial disordered state bifurcates into a fully synchronous

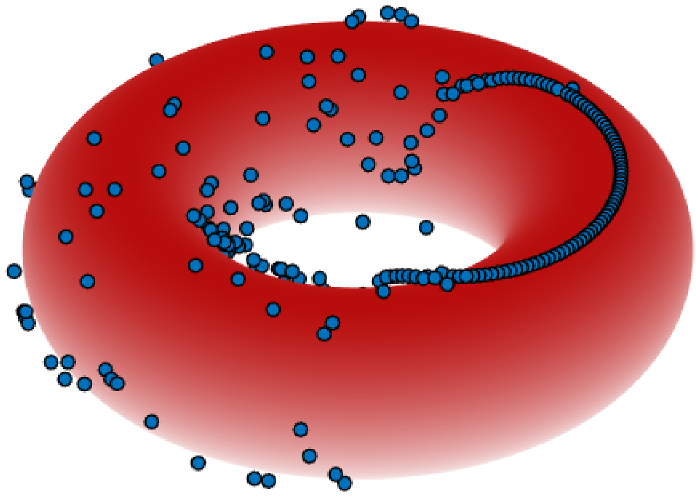

Figure 5.3: A snap shot of a chimera state (as in Fig. 5.2) shown on a torus. Azinuthal angle represents spatial position on the ring (index-n), and each line of latitude on the torus represents constant phase. Here $N = 250$, $\alpha = 1.37$, $A = 0.95$.

state that remains stable for some time. A chimera state is born an remains in existence for a brief time which in turn re-forms into complete synchronisation. This synchronous state is the lost and disorder remains for the time.

In Figures 5.5(a,b) the initial disordered state bifurcates into a chimera synchronised state almost immediately and remains stable for an extended period. In both cases a fully synchronous state emerges followed by a disordered state. When a chimera state is formed it is interesting to see that it the synchronous state remains localised in space but the degree of synchronisation, $R(x)$, displays some oscillation in time.

Finally, in Figure 5.5(d), the initial disordered state bifurcates after some time into complete synchronisation that remains stable for finite time. The synchronous state is then lost to disorder for the remaining time.

These four integrations are not special and display typical examples of the wide variety of the dynamics of the system (5.4) where the only difference in each case is the random distribution of the initial phases. In this short exploration it has not been possible to explore the full range of parameter space and initial conditions to enable an understanding the emergence and stability of the chimera. In fact it has raised more questions than it has answered.

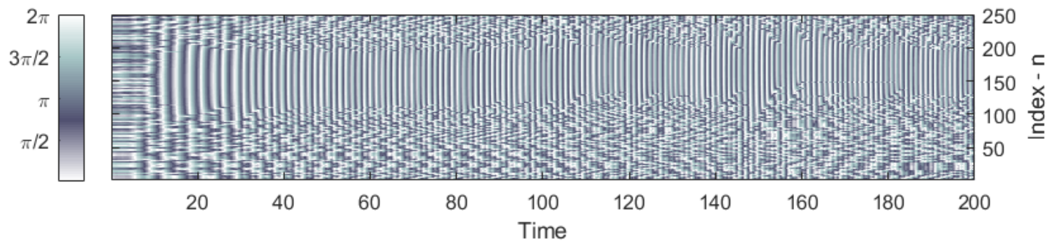

(a)

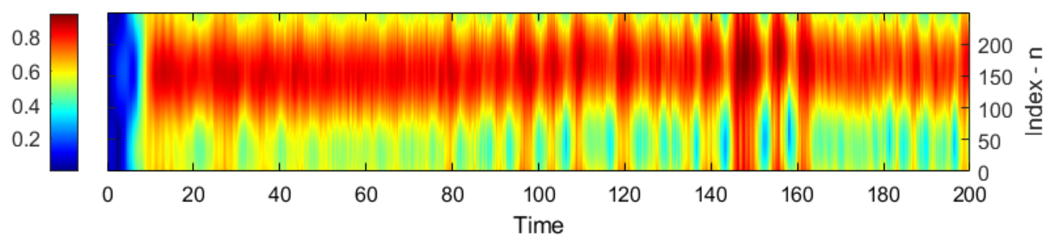

(b)

Figure 5.4: A typical integrations of (5.4) with $\alpha = 1.37$, $A = 0.95$, $t = 200$, $N = 250$. (a) shows the evolution of the distribution of phase on the ring. Index - n is the spatial variable x and specifies the location on the ring network. In (b) the evolution of the spatial order parameter, $R(x, t)$ is shown. Colour coded is its magnitude, with blue signifying incoherence and red signifying coherence. A chimera state is born at around $t = 7$ and remains for the entire length of the integration. There are clear oscillations in space and time.

With further numerical and analytical work some further questions could be explored. In what regions of the parameter space (A, α) do chimeras form? What are the basins of attraction? Can chimeras been born out of both disordered and synchronous states, particularly as the synchronous state is stable? What is the nature of the bifurcation from disordered state to chimera? How are chimeras born and how do they die? Globally synchronous states depend on network structure, what about chimeras? Do stable chimeras exists or are they always transient as seen here?

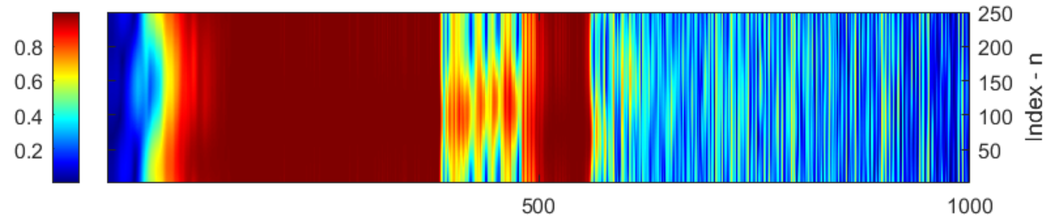

(a)

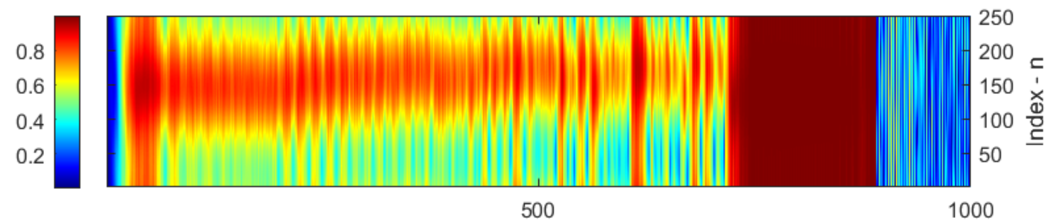

(b)

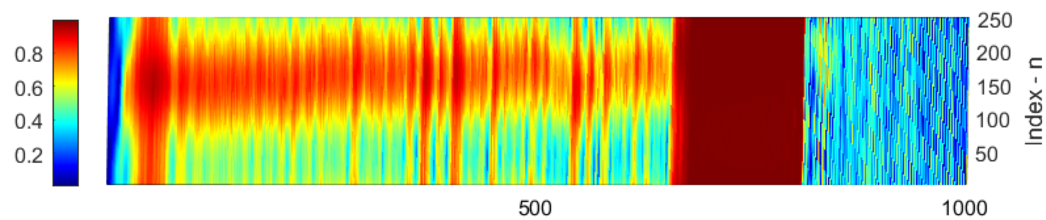

(c)

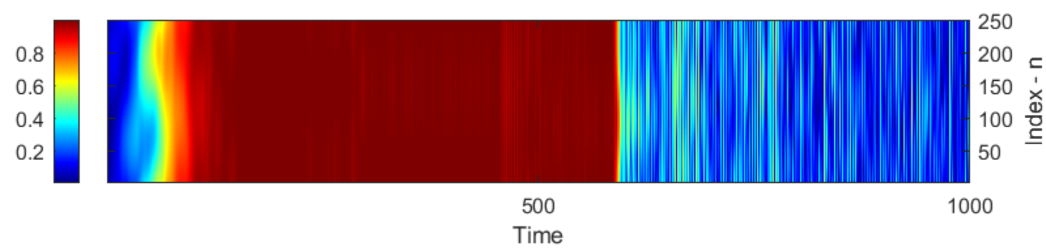

(d)

Figure 5.5: Four typical integrations of (5.4) with $\alpha = 1.37$, $A = 0.95$, $t = 1000$, $N = 250$. Colour coded is the magnitude of the spatial order parameter, $R(x,t)$, with blue signifying incoherence and red signifying coherence. Index - n is the spatial variable x and specifies the location on the ring network. Chimera states can be seen in (a),(b) and (c) and can be seen to oscillate in both space and time, although they do not survive for the entire integration time. In each case they die and a fully synchronous state is born. The only quantity varying in each run is the randomisation of initial phases.

Chapter 6

Summary and further work

We have explored the globally coupled Kuramoto model both analytically and numerically and have seen that this fundamental model is able to produce synchronisation in a finite population of oscillators. The numerical results compare well with the predications from theoretical analysis in the continuum limit. We further considered the Kuramoto-Sakaguchi model with phase shifted coupling. Numerical exploration on a ring network with non-local coupling revealed interesting chimera states where both incoherent and synchronous states coexist and a brief look at the long term behaviour suggest that these states may not be stable in the long term.

There are numerous avenues that can be explored when considering extending this work. We have assumed that the distribution of natural frequencies $g(\omega)$ is both symmetric and unimodal. It would be interesting to examine the effect of *asymmetry* on the dynamics. The main difficulty will be in constructing, self-consistently, the equations describing the mean field. A starting point would be the work of (Martens et al., 2009) who consider bimodal frequency distributions. We considered initially the dynamics of globally (or all to all) coupled oscillators on a complete network. It would be interesting to examine the role of the *network connectivity* to see whether synchronisation occurs with reduced connectivity. This is still unanswered, but (Townsend et al., 2020) investigate this problem for identical oscillators and suggest that the critical connectivity may be 75%.

In searching for chimera states in the Kuramoto-Sakaguchi model we considered the dynamics on a one-dimension ring with non local coupling. It would be worthwhile extending this to *two-dimensional array networks* where interesting pattern formation, phase and frequency spirals are observed (Kim et al., 2004; Ottino-Löffler and Strogatz, 2016; Shima and Kuramoto, 2004). Alternatively we could remain with all-to-all coupling but introduce an *inhomogeneous coupling* strength (Ko and Ermentrout, 2008). Chimera states have also been observed on two sub-networks that are coupled together with all-to-all coupling within each network (Abrams and Strogatz, 2006; Laing, 2009).

In attempting to apply these abstract mathematical models to real-world phenomena we would need to move away from the simple, but rich structure of the simple Kuramoto-Sakaguchi model and modify the dynamics somewhat.

One modification that has been extensively explored is a noisy or *stochastic* model. This is the standard Kuramoto model with a white noise term added. The first to consider this was Sakaguchi (1988) and there has been a great deal of research ever since (Acebrón et al., 2005).

One observation with the first-order models considered in this work is that they tend to approach synchronization more rapidly than is observed in practice, particularly in biological systems. They also require infinite coupling strength to achieve full synchronisation. Introducing an *inertia* term into the dynamics can solve these issues. The addition of inertia makes the model second-order by introduction a $\ddot{\theta}$ into the model, in effect giving the oscillators a 'mass'. The second-order model has many applications including synchronisation in power grids (Filatrella et al., 2008).

One of the most natural modifications to a Kuramoto model is the introduction of *time-delayed* coupling. In biological an physical systems signals propagate at finite speed and transmission delay between oscillators is to be expected. Time delayed coupling changes the dynamics substantially (Yeung and Strogatz, 1999; Lee et al., 2009).

Finally, an exciting new avenue of research has opened up into oscillators that synchronise in phase as well as self-organise in space through a coupling of phase and spatial dynamics. This brings together two historically unrelated areas of research, namely synchronisation and swarming or flocking (of birds, insects or fish for example). O'Keeffe et al. (2017) call these oscillators that both synchronise and swarm "*swarmalators*", and this seems to be fascinating area worth pursuing.

References

Abrams, D. M., Mirollo, R., Strogatz, S. H. and Wiley, D. A. (2008), 'Solvable model for chimera states of coupled oscillators', *Phys. Rev. Lett.* **101**(8), 1–4.

Abrams, D. M. and Strogatz, S. H. (2004), 'Chimera states for coupled oscillators', *Phys. Rev. Lett.* **93**(17), 1–4.

Abrams, D. M. and Strogatz, S. H. (2006), 'Chimera states in a ring of nonlocally coupled oscillators', *Int. J. Bifurc. Chaos* **16**(1), 21–37.

Acebrón, J. A., Bonilla, L. L., Vicente, C. J., Ritort, F. and Spigler, R. (2005), 'The Kuramoto model: A simple paradigm for synchronization phenomena', *Rev. Mod. Phys.* **77**(1), 137–185.

Blackbeard, N., Wieczorek, S., Erzgräber, H. and Dutta, P. S. (2014), 'From synchronisation to persistent optical turbulence in laser arrays', *Phys. D Nonlinear Phenom.* **286-287**, 43–58.

Buck, J. (1988), 'Synchronous Rhythmic Flashing of Fireflies. II.', *Q. Rev. Biol.* **63**(3), 265–289.

Filatrella, G., Nielsen, A. H. and Pedersen, N. F. (2008), 'Analysis of a power grid using a Kuramoto-like model', *Eur. Phys. J. B* **61**(4), 485–491.

Gherardini, S., Gupta, S. and Ruffo, S. (2018), 'Spontaneous synchronisation and nonequilibrium statistical mechanics of coupled phase oscillators', *Contemp. Phys.* **59**(3), 229–250.

Gray, C. M. (1994), 'Journal of Computational Neuroscience volume', *J. Comput. Neurosci.* **1**, 11–38.

Gupta, S., Campa, A. and Ruffo, S. (2014), 'Kuramoto model of synchronization: equilibrium and nonequilibrium aspects', *J. Stat. Mech. Theory Exp.* **2014**(6), 1–12.

Gupta, S., Campa, A. and Ruffo, S. (2018), *Statistical Physics of Synchronization*, Springer Briefs in Complexity.

Ha, S. Y., Li, Z. and Xue, X. (2013), 'Formation of phase-locked states in a population of locally interacting Kuramoto oscillators', *J. Differ. Equ.* **255**(10), 3053–3070.

Huygens, C. (1967), *Evres Complete, Volume 15*, Swets and Zeitlinger B.V., Amsterdam.

Izhikevich, E. M. (2007), *Dynamical Systems in Neuroscience*, Vol. 25, MIT Press.

Kim, P. J., Ko, T. W., Jeong, H. and Moon, H. T. (2004), 'Pattern formation in a two-dimensional array of oscillators with phase-shifted coupling', *Phys. Rev. E - Stat. Physics, Plasmas, Fluids, Relat. Interdiscip. Top.* **70**(065201), 1–4.

Ko, T.-W. and Ermentrout, B. (2008), 'Partially Locked States in Coupled Oscillators due to Inhomogeneous Coupling', *Phys. Rev. E* **78**(1), 016203.

Kuramoto, Y. (1975), Self-entrainment of a population of coupled non-linear oscillators, *in* H. Arakai, ed., 'Int. Symp. Math. Probl. Theor. Phys.', p. 420.

Kuramoto, Y. (1983), *Chemical Oscillations, Waves and Turbulence.*, Spinger-Verlag, New York.

Kuramoto, Y. and Battogtokh, D. (2002), 'Coexistence of Coherence and Incoherence in Nonlocally Coupled Phase Oscillators', *Nonlinear Phenom. Complex Syst.* **4**, 380–385.

Kuramoto, Y. and Nishikawa, I. (1987), 'Statistical macrodynamics of large dynamical systems. Case of a phase transition in oscillator communities', *J. Stat. Phys.* **49**, 569–605.

Kuramoto, Y. and Nishikawa, I. (1988), Onset of Collective Rhythms in Large Poulations of of Couple Oscillators, *in* H. Takayama, ed., 'Coop. Dyn. Complex Phys. Syst.', Spinger, Berlin, p. 300.

Laing, C. R. (2009), 'The dynamics of chimera states in heterogeneous Kuramoto networks', *Phys. D Nonlinear Phenom.* **238**(16), 1569–1588.

Lee, W. S., Ott, E. and Antonsen, T. M. (2009), 'Large Coupled Oscillator Systems with Heterogeneous Interaction Delays', *Phys. Rev. Lett.* **103**(4), 044101.

MacKay, W. A. (1997), 'Synchronized neuronal oscillations and their role in motor processes', *Trends Cogn. Sci.* **1**(5), 176–183.

Martens, E. A., Barreto, E., Strogatz, S. H., Ott, E., So, P. and Antonsen, T. M. (2009), 'Exact results for the Kuramoto model with a bimodal frequency distribution', *Phys. Rev. E - Stat. Nonlinear, Soft Matter Phys.* **79**(2), 1–28.

Martens, E. A., Laing, C. R. and Strogatz, S. H. (2010), 'Solvable model of spiral wave chimeras', *Phys. Rev. Lett.* **104**(4), 1–4.

Néda, Z., Ravasz, E., Vicsek, T., Brechet, Y. and Barabási, A. L. (2000), 'Physics of the rhythmic applause', *Phys. Rev. E - Stat. Physics, Plasmas, Fluids, Relat. Interdiscip. Top.* **61**(6B), 6987–6992.

O'Keeffe, K. P., Hong, H. and Strogatz, S. H. (2017), 'Oscillators that sync and swarm', *Nat. Commun.* **8**(1), 1–12.

Ott, E. and Antonsen, T. M. (2008), 'Low dimensional behavior of large systems of globally coupled oscillators', *Chaos* **18**(3), 1–16.

Ott, E. and Antonsen, T. M. (2009), 'Long time evolution of phase oscillator systems', *Chaos* **19**(2).

Ottino-Löffler, B. and Strogatz, S. H. (2016), 'Frequency spirals', *Chaos* **26**(9), 1–10.

Pazó, D. (2005), 'Thermodynamic limit of the first-order phase transition in the Kuramoto model', *Phys. Rev. E - Stat. Nonlinear, Soft Matter Phys.* **72**(4).

Pikovsky, A., Rosenblum, M. and Kurths, J. (2001), *Synchronization: A Universal Concept in Nonlinear Sciences*, 12 edn, Cambridge Univeristy Press, Cambridge.

Rodrigues, F. A., Peron, T. K., Ji, P. and Kurths, J. (2016), 'The Kuramoto model in complex networks', *Phys. Rep.* **610**, 1–98.

Rohden, M., Sorge, A., Timme, M. and Witthaut, D. (2012), 'Self-organized synchronization in decentralized power grids', *Phys. Rev. Lett.* **109**(6), 1–5.

Sakaguchi, H. (1988), 'Cooperative Phenomena in Coupled Oscillator Systems under External Fields', *Prog. Theor. Phys.* **79**(1), 39–46.

Sakaguchi, H. and Kuramoto, Y. (1986), 'A soluble active rotator model showing phase transitions via mutial entrainment', *Prog. Theor. Phys.* **76**(3), 576–581.

Shima, S. I. and Kuramoto, Y. (2004), 'Rotating spiral waves with phase-randomized core in nonlocally coupled oscillators', *Phys. Rev. E - Stat. Nonlinear, Soft Matter Phys.* **69**(3).

Strogatz, S. H. (2000), 'From Kuramoto to Crawford: exploring the onset of synchronization in populations of coupled oscillators', *Phys. D Nonlinear Phenom.* **143**, 1–20.

Strogatz, S. H. (2004), *Sync: The Emerging Science of Spontaneous Order*, Penguin.

Strogatz, S. H. and Mirollo, R. E. (1991), 'Stability of incoherence in a population of coupled oscillators', *J. Stat. Phys.* **63**(3-4), 613–635.

Strogatz, S. H. and Stewart, I. (1993), 'Coupled oscillators and biological synchronization', *Sci. Am.* **269**(6), 102–109.

Townsend, A., Stillman, M. and Strogatz, S. H. (2020), 'Dense networks that do not synchronize and sparse ones that do', *Chaos* **30**, 083142.

van Hemmen, J. L. and Wreszinski, W. F. (1993), 'Lyapunov function for the Kuramoto model of nonlinearly coupled oscillators', *J. Stat. Phys.* **72**(1-2), 145–166.

Watanabe, S. and Strogatz, S. H. (1993), 'Integrability of a globally coupled oscillator array', *Phys. Rev. Lett.* **70**, 2391.

Wiener, N. (1958), *Nonlinear Problems in Random Theory*, MIT Press, Cambridge, MS.

Wiener, N. (1961), *Cybernetics: Or Control and Communication in the Animal and the Machine*, 2 edn, MIT Press, Cambridge, MA.

Winfree, A. T. (1967), 'Biological rhythms and the behaviour of populations of coupled oscillators', *Theor. Biol.* **16**(1), 15–42.

Winfree, A. T. (2001), *The Geometry of Biological Time*, 2 edn, Springer-Verlag, New York.

Yeung, M. and Strogatz, S. H. (1999), 'Time Delay in the Kuramoto Model of Coupled Oscillators', *Phys. Rev. Lett.* **82**(3), 648–651.